Orientations and Phase Transformations

27-750

Texture, Microstructure & Anisotropy

Ben Anglin

Acknowledgment to S. Mandal for slides on Ti

Last revised 23 Apr. 2014

Objective

- Understand orientation relationships
- Be able to construct misorientation matrices from given orientation relationship
- Find variant orientations from orientation relationship

References

- Phase Transformations in Metals and Alloys, D.A. Porter and K.E. Easterling
- Worked examples in the geometry of crystals, H.K.D.H. Bhadeshia

Orientation Relationships

- Orientation Relationship (OR): Relation between specific planes and directions of two crystals on either side of boundary.
- During most phase transformations, some favored orientation relationship exists between the parent and the product phases which allows the best fit at the interface between the two crystals.
- Why important? Phase transformations; morphology of precipitates; nucleation mechanisms; interfaces; high temperature orientation determination; thin film orientation prediction.

*Slide courtesy of S Mandal

First, we need to look at interfaces in general

- Coherent: two crystal match perfectly across boundary, regardless of chemical composition (may include small *coherency strains*)
- Semi-coherent: slight mismatch in crystals, replacing coherency strains with *coherency dislocations*
- Incoherent: two crystals with very different atomic configurations

The Basics

Notation:

$$(hkl)_{\alpha}//(h'k'l')_{\beta} \qquad [uvw]_{\alpha}//[u'v'w']_{\beta}$$

The (hkl) plane of the α crystal lies parallel to the (h'k'l') plane of the β crystal

Similarly for the [uvw] and [u'v'w'] directions of the two crystals

[uvw] and [u'v'w'] must lie in the (hkl) and (h'k'l') planes, respectively

The orientation relationship holds regardless of the coherency of the boundary

The Basics

Precipitates have lower energy if surrounded by low-energy coherent interfaces.

Wulff construction from interfacial energy plot to find possible coherent interfaces – flat and planar. Typically terminated by incoherent interfaces on ends.

Flat, planar coherent interfaces are called *habit planes.* These are NOT necessarily the same as the parallel planes in the OR definition.

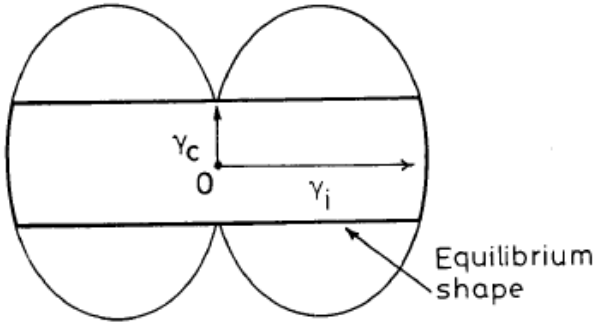

Fig. 3.40 A section through a γ-plot for a precipitate showing one coherent or semicoherent interface, together with the equilibrium shape (a disc).

NB: precipitate shapes may vary due to coherency strains, grain growth, and other anisotropic effects.

Widmanstätten morphology

- Widmanstätten's name is associated with platy precipitates that possess a definite crystallographic relationship with their parent phase.
- Examples:
  - ferrite in austenite (iron-rich meteors!)
  - γ' precipitates in Al-Ag (see fig. 3.42)
  - hcp Ti in bcc Ti (two-phase Ti alloys, slow cooled)
  - θ' precipitates in Al-Cu
- The latter example is based on the orientation relationship $(001)_{\theta'}//\{001\}_{Al}$, $[100]_{\theta'}//<100>_{Al}$. See fig. 3.41 for a diagram of the tetragonal structure of θ' whose *a*-*b* plane, i.e. (001), aligns with the (100) plane of the parent Al.

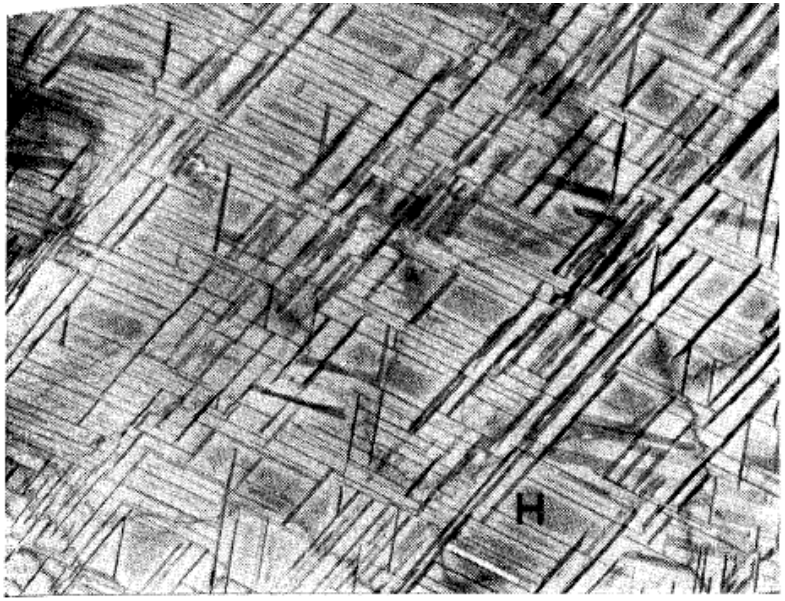

Fig. 3.42 Electron micrograph showing the Widmanstätten morphology of γ' precipitates in an Al-4 atomic % Ag alloy. GP zones can be seen between the γ', e.g. at H (× 7000). (R.B. Nicholson and J. Nutting, *Acta Metallurgica*, **9** (1961) 332.)

*Slide courtesy of AD Rollett

The Basics

Orientation relationships describe the specific orientation between two crystals

This is usually done for phase boundaries, but can describe grain boundaries as well.

Can you think of a special grain boundary that has a well-known orientation relationship?

$$(111)_\alpha // (111)_\beta$$
$$[01\bar{1}]_\alpha // [\bar{1}10]_\beta$$

The $\Sigma 3$ CSL boundary has this OR. What is the habit plane if this is a coherent $\Sigma 3$? {111}

Some common ORs

Bagaryatsky OR

$[1\ 0\ 0]_{cem} \,||\, [0\ -1\ 1]_{fer}$

$[0\ 0\ 1]_{cem} \,||\, [-1\ -1\ 2]_{fer}$

Between cementite and ferrite phases in Pearlite.

Kurdjumov-Sachs OR

$\{111\}_{FCC} \,||\, \{0\ 1\ 1\}_{BCC}$

$\langle 101 \rangle_{FCC} \,||\, \langle 1\ 1\ 1 \rangle_{BCC}$

Between austenite and ferrite phases in Iron; Cu-Zn.

Burgers OR

$(0\ 0\ 0\ 1)_{HCP} \,||\, \{0\ 1\ 1\}_{BCC}$

$[1\ 1\ -2\ 0]_{HCP} \,||\, \langle 1\ 1\ 1 \rangle_{BCC}$

Between alpha and beta phases in Ti, Zr.

Potter OR

$(0\ 1\ -1\ 1)_{HCP} \,||\, \{-1\ 0\ 1\}_{BCC}$

$[2\ -1\ -1\ 0]_{HCP} \,||\, \langle 1\ -1\ 1 \rangle_{BCC}$

Between alpha and beta phases in Mg-Al aloys.

*Slide courtesy of S Mandal

Complex semi-coherent interfaces

- It can often happen that an orientation relationship exists despite the lack of an exact match.
- Such is the case for the relationship between bcc and fcc iron (ferrite and austenite).

Note limited atomic match for the NW relationship

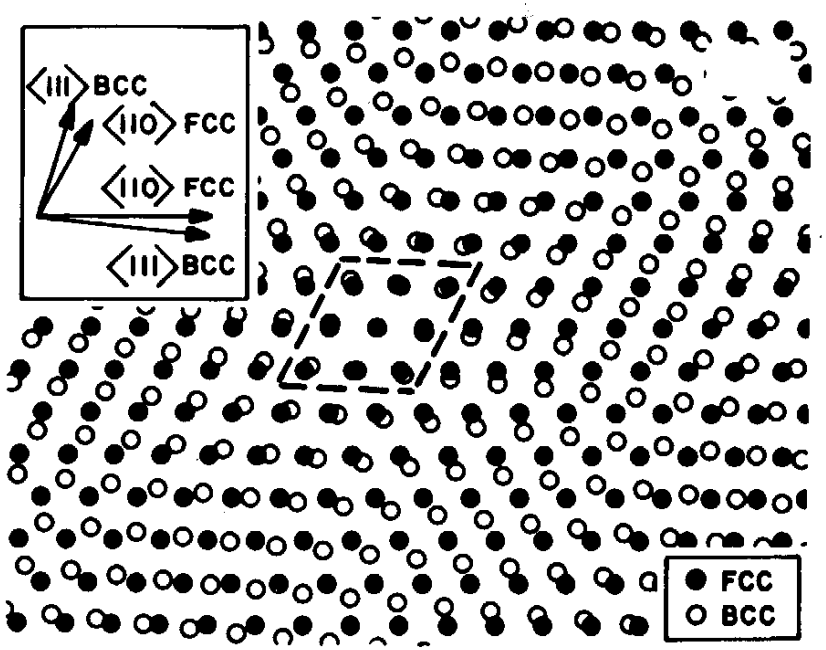

Fig. 3.38 Atomic matching across a $(111)_{fcc}/(110)_{bcc}$ interface bearing the NW orientation relationship for lattice parameters closely corresponding to the case of fcc and bcc iron (M.G. Hall *et al.*, *Surface Science*, **31** (1972) 257).

*Slide courtesy of AD Rollett

Orientation relationships in iron

- There are two well-known orientation relationships for fcc-bcc iron.
- The Nishiyama-Wasserman (NW) relationship is specified as $\{110\}_{bcc}/\{111\}_{fcc}$, $<001>_{bcc}//<101>_{fcc}$.
- The NW relationship only gives good atomic fit in 8% of the boundary area.
- The Kurdjumov-Sachs (KS) relationship is specified as $\{110\}_{bcc}/\{111\}_{fcc}$, $<111>_{bcc}//<101>_{fcc}$.
- These two differ by only a 5.6° rotation in the interface plane.
- Better atomic matching is possible for irrational planes used.

*Slide courtesy of AD Rollett

Creating Coordinate Transformation Matrix for OR

Let's say you are given an orientation relationship and you want to know the rotation and change in volume between the two crystals. The coordinate transformation matrix, *J*, contains both pieces of information.

Given: $(hkl)_\alpha // (h'k'l')_\beta$, $[uvw]_\alpha // [u'v'w']_\beta$

First, define which phase is the parent phase and which is the derivative phase (e.g. $\alpha \rightarrow \beta$)

Define:

$$m = \left| \begin{pmatrix} h & k & l \end{pmatrix}_\alpha \right| / \left| \begin{pmatrix} h' & k' & l' \end{pmatrix}_\beta \right|$$

$$k = \left| \begin{bmatrix} u & v & w \end{bmatrix}_\alpha \right| / \left| \begin{bmatrix} u' & v' & w' \end{bmatrix}_\beta \right|$$

$$g = \left| \begin{bmatrix} r & s & t \end{bmatrix}_\alpha \right| / \left| \begin{bmatrix} r' & s' & t' \end{bmatrix}_\beta \right|$$

Where did $[rst]_\alpha$ and $[r's't']_\beta$ come from?

Can either be specified in OR or found by cross product of normal vector, *n*, for (hkl) and direction vector, *b*, for [uvw]. (See earlier lectures for defining orientation matrix from (hkl)[uvw].)

***k*, *m,* and *g* relate the length of the lattice vectors of the two crystals.

Creating Coordinate Transformation Matrix for OR

Recall from previous lectors, each column represents the components of a basis vector of α in β, in [uvw], [rst], (hkl) order.

To find J for α→β:

$$\begin{pmatrix} u'\cdot k & r'\cdot g & h'\cdot m \\ v'\cdot k & s'\cdot g & k'\cdot m \\ w'\cdot k & t'\cdot g & l'\cdot m \end{pmatrix}_{\beta} = J \times \begin{pmatrix} u & r & h \\ v & s & k \\ w & t & l \end{pmatrix}_{\alpha}$$

$$J = \begin{pmatrix} u'\cdot k & r'\cdot g & h'\cdot m \\ v'\cdot k & s'\cdot g & k'\cdot m \\ w'\cdot k & t'\cdot g & l'\cdot m \end{pmatrix} \times \begin{pmatrix} u & r & h \\ v & s & k \\ w & t & l \end{pmatrix}^{-1}$$

Coordinate Transformation Matrix for OR to Strain and Rotation Matrices

Within the transformation matrix are stretch, *P*, and rotation, *U*, matrices. When multiplied together these matrices recover the transformation matrix. *J=UP*

To find the stretch and rotation matrices use a *polar decomposition†*.

$P = \sqrt{J^* J}$, J^* denotes the conjugate transpose of J

and $U = J \cdot P^{-1}$

Per usual, transform rotation matrix, *U*, to other notations for other uses

Use MATLAB (function "poldec") or some other computation package to make this calculation easier

†See, e.g., An Introduction to Continuum Mechanics, M. Gurtin

Coordinate Transformation Matrix for OR to Strain and Rotation Matrices (Example)

Given the Kurdjumov-Sachs OR for ferrite, α, and austenite, γ, below, find the rotation matrix.

$[1\ \ 1\ \ 1]_\gamma \parallel [0\ \ 1\ \ 1]_\alpha \qquad [\bar{1}\ \ 0\ \ 1]_\gamma \parallel [\bar{1}\ \ \bar{1}\ \ 1]_\alpha \qquad [1\ \ \bar{2}\ \ 1]_\gamma \parallel [2\ \ \bar{1}\ \ 1]_\alpha$

$$k = a_\gamma\sqrt{3} \Big/ a_\alpha\sqrt{2} \qquad g = a_\gamma\sqrt{2} \Big/ a_\alpha\sqrt{3} \qquad m = a_\gamma\sqrt{6} \Big/ a_\alpha\sqrt{6} = a_\gamma \Big/ a_\alpha$$

$$\begin{pmatrix} 0 & \bar{g} & 2m \\ k & \bar{g} & \bar{m} \\ k & g & m \end{pmatrix} = J \times \begin{pmatrix} 1 & \bar{1} & 1 \\ 1 & 0 & \bar{2} \\ 1 & 1 & 1 \end{pmatrix}$$

$$J = \frac{1}{6}\begin{pmatrix} 3g+2m & \bar{4}m & \bar{3}g+2m \\ 2k+3g-m & 2k+2m & 2k-3g-m \\ 2k-3g+m & 2k-2m & 2k+3g+m \end{pmatrix}$$

Coordinate Transformation Matrix for OR to Strain and Rotation Matrices (Example)

Given: $a_\alpha = 0.28662$ nm $\qquad a_\gamma = 0.36551$ nm

$$J = \begin{pmatrix} 0.9457 & -0.8502 & -0.0955 \\ 0.8287 & 0.9457 & -0.2125 \\ 0.2125 & 0.0955 & 1.2538 \end{pmatrix}$$

Polar Decomposition

Rotation

$$U = \begin{pmatrix} 0.7416 & -0.6667 & -0.0749 \\ 0.6598 & 0.7416 & -0.1667 \\ 0.1667 & 0.0749 & 0.9832 \end{pmatrix}$$

Stretch

$$P = \begin{pmatrix} 1.2752 & 0.0000 & 0.0000 \\ 0.0000 & 1.2752 & 0.0000 \\ 0.0000 & 0.0000 & 1.2752 \end{pmatrix}$$

Strain = $P - 1$

Creating Misorientation Matrix for OR

Let's say your MATLAB is broken (PANIC!), or you simply don't like polar decompositions. How else can we calculate the misorientation matrix for an OR?

$$\begin{bmatrix} u & v & w \end{bmatrix}_\alpha \parallel \begin{bmatrix} u' & v' & w' \end{bmatrix}_\beta \qquad \begin{pmatrix} h & k & l \end{pmatrix}_\alpha \parallel \begin{pmatrix} h' & k' & l' \end{pmatrix}_\beta$$

Assume: (hkl) // (h'k'l') // ND
and [uvw] // [u'v'w'] // RD

1.) Construct orientation matrix for phase α.

$$g_\alpha = \begin{pmatrix} b_1 & t_1 & n_1 \\ b_2 & t_2 & n_2 \\ b_3 & t_3 & n_3 \end{pmatrix}$$

2.) Construct orientation matrix for phase β.

$$g_\beta = \begin{pmatrix} b'_1 & t'_1 & n'_1 \\ b'_2 & t'_2 & n'_2 \\ b'_3 & t'_3 & n'_3 \end{pmatrix}$$

3.) Compute misorientation matrix from one phase to the other.

$$\Delta g = g_\beta g_\alpha^{-1}$$

Creating Misorientation Matrix for OR

What about ORs where a relative angle is specified? For example, a common OR in pearlite is the Pitsch-Petch OR.

$$[1\ 0\ 0]_\theta \ 2.6^\circ \text{ from } [\bar{3}\ 1\ \bar{1}]_\alpha$$
$$[0\ 1\ 0]_\theta \ 2.6^\circ \text{ from } [1\ 3\ 1]_\alpha$$
$$(0\ 0\ 1)_\theta \parallel (2\ 1\ \bar{5})_\alpha$$

Assume (hkl) // (h'k'l') // ND and [uvw] // [u'v'w']] // RD (ignore angle difference initially)

1.) Construct orientation matrix for phase θ.

$$g_\theta = \begin{pmatrix} 1 & 0 & 0 \\ 0 & 1 & 0 \\ 0 & 0 & 1 \end{pmatrix}$$

2.) Construct orientation matrix for phase α.

$$g_\alpha = \begin{pmatrix} -3/\sqrt{11} & 4/\sqrt{330} & 2/\sqrt{30} \\ 1/\sqrt{11} & 17/\sqrt{330} & 1/\sqrt{30} \\ -1/\sqrt{11} & 5/\sqrt{330} & -5/\sqrt{30} \end{pmatrix}$$

3.) Compute misorientation matrix from one phase to the other. $\Delta g^* = g_\alpha g_\theta^{-1}$

4.) Construct rotation matrix for small angle. $\hat{r} = \left\langle 2/\sqrt{30} \quad 1/\sqrt{30} \quad -5/\sqrt{30} \right\rangle, \ \alpha = 2.6^\circ \rightarrow g_{2.6^\circ}$

5.) Combine rotations. $\Delta g = g_{2.6^\circ} \Delta g^*$

Creating Misorientation Matrix for OR

Check if the misorientation matrix is correct by plotting a discrete pole figure of the relevant poles and computing angular difference between poles with small angle deviation.

Bagaryatsky

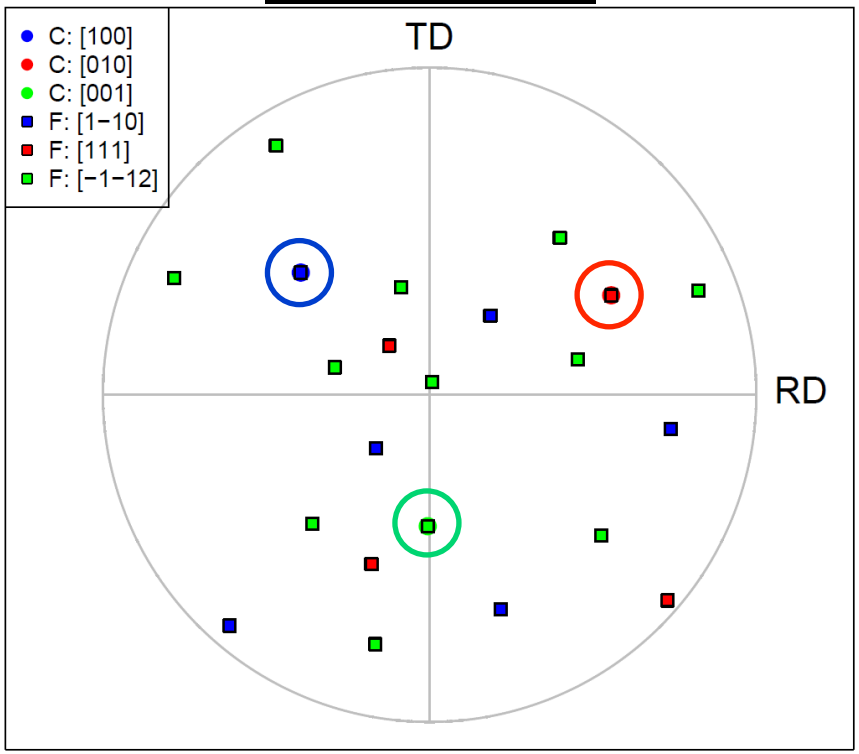

Angular distances:
b-axis: 0.00015°
a-axis:0.000094°
c-axis: 0.000072°

Pitsch-Petch

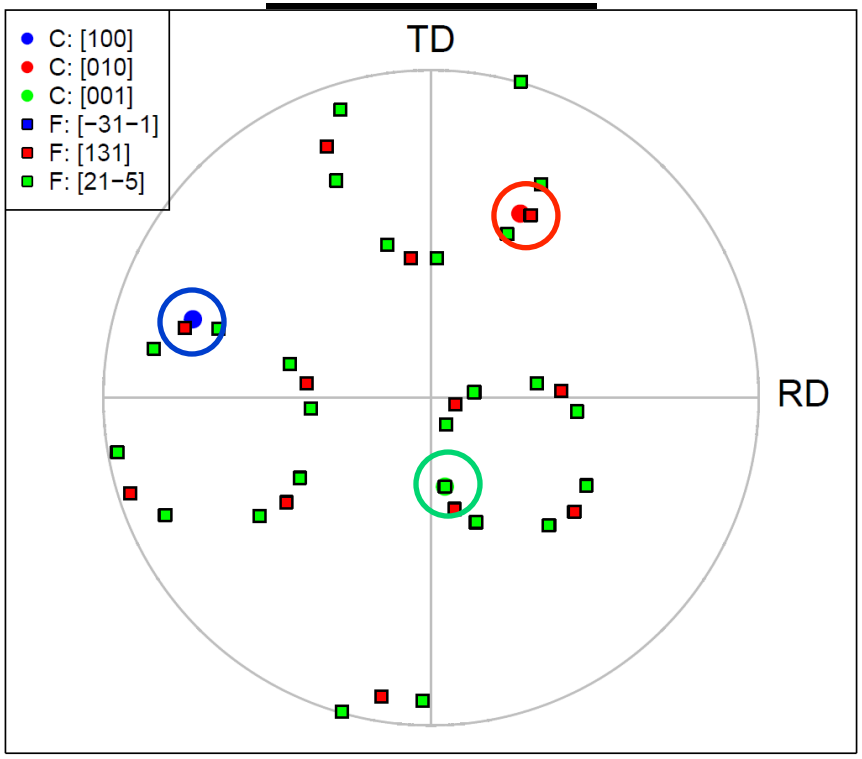

Angular distances:
b-axis: 2.608235°
a-axis: 2.607674°
c-axis: 0.000065°

ORs and Crystal Symmetry

What role do crystal symmetry operators play in the determination of precipitate orientations from parent orientation?

Symmetrically equivalent misorientations are computed by:

$$\Delta g = O_c^{\beta} g_{\beta} g_{\alpha}^{-1} O_c^{\alpha}$$

Bagaryatsky OR: BCC = 24 equivalent, Orthorhombic = 8 equivalent

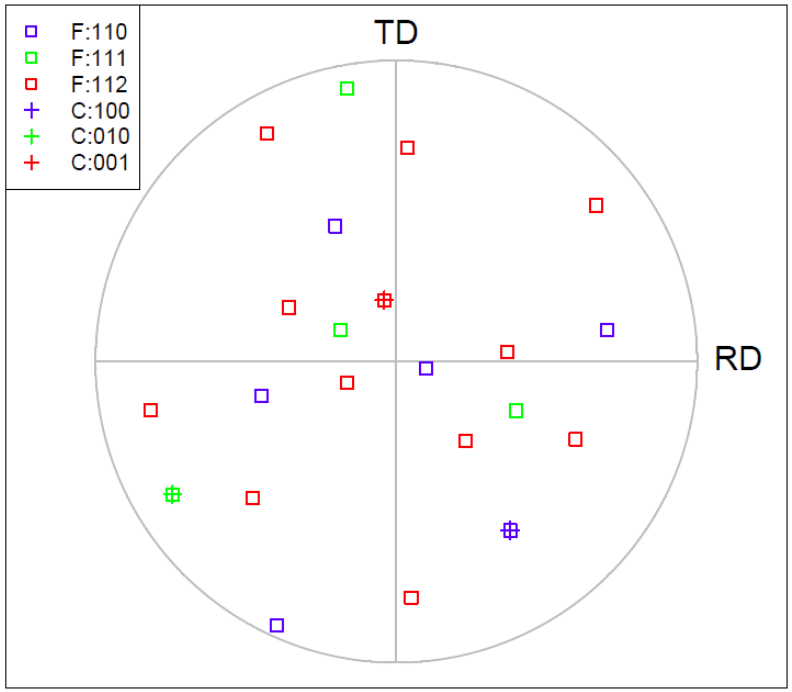

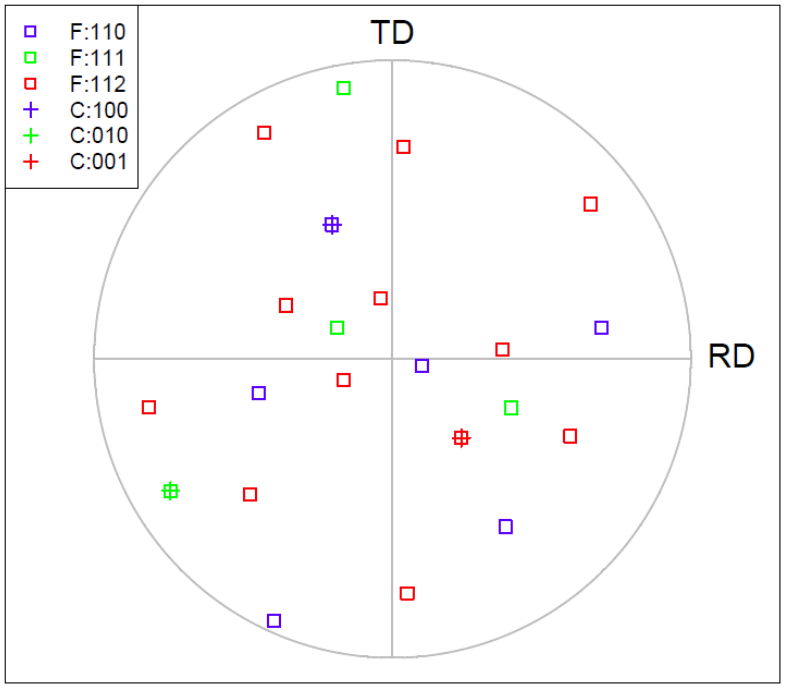

ORs and Crystal Symmetry (example)

Objective: build representative microstructure as a result of phase transformation, with real ORs (e.g. pearlite)

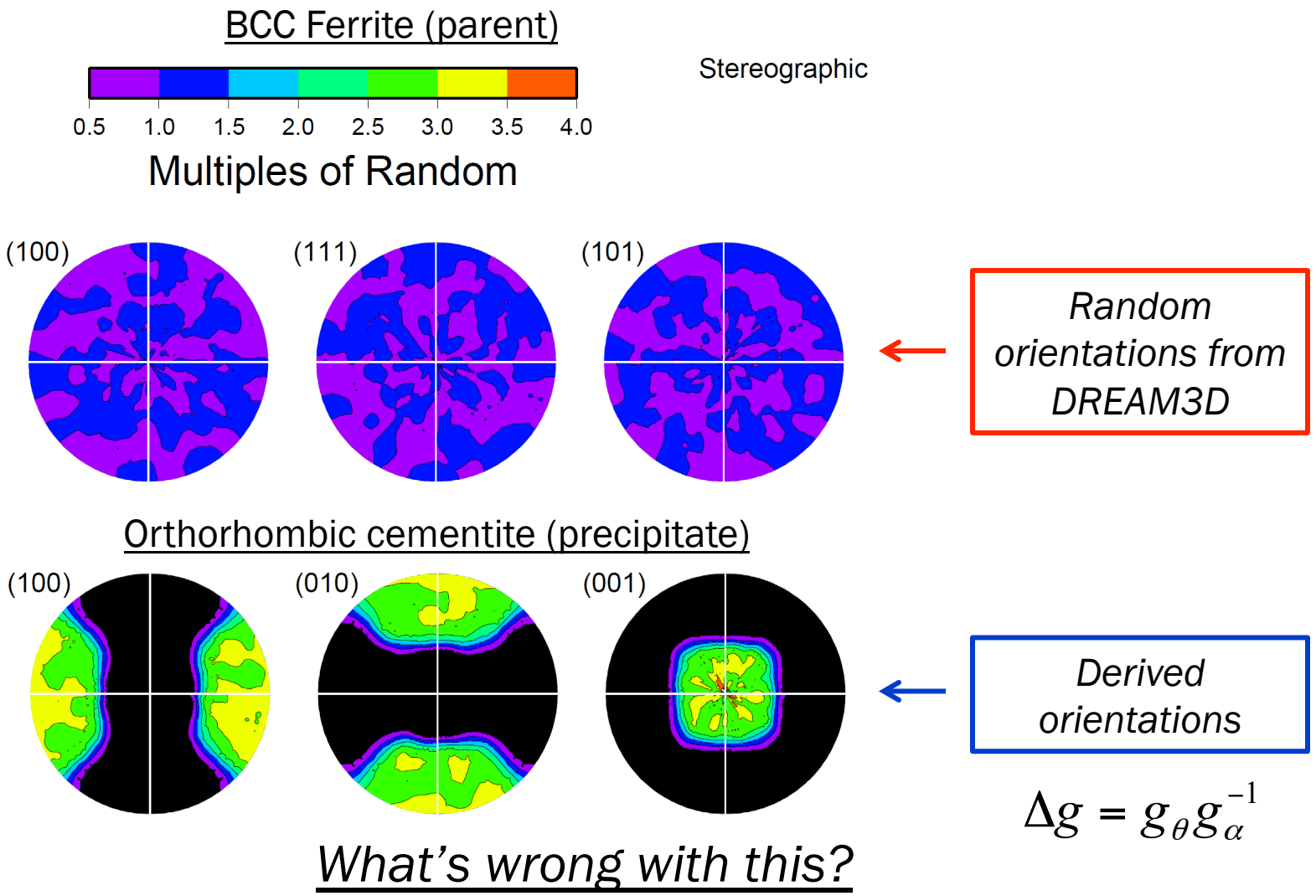

ORs and Crystal Symmetry (example)

Plot discrete pole figures of DREAM3D orientations to see where symmetry is applied (in DREAM3D or left to user during plotting)

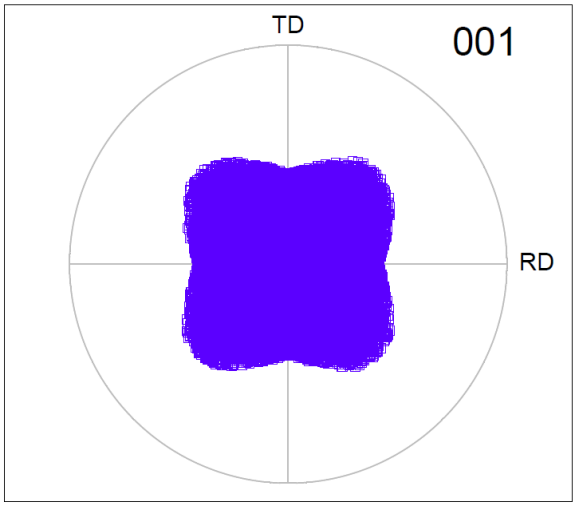

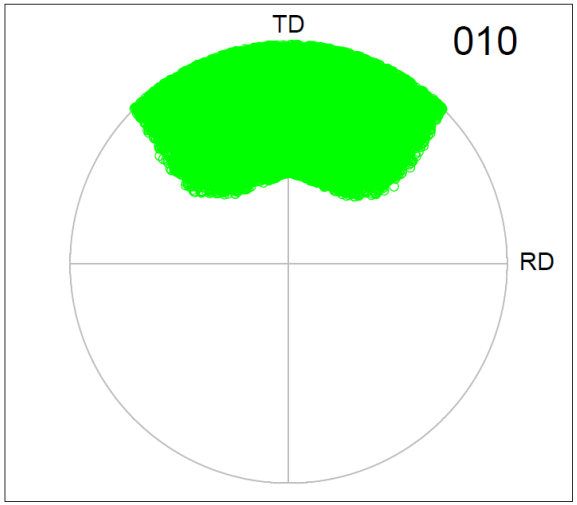

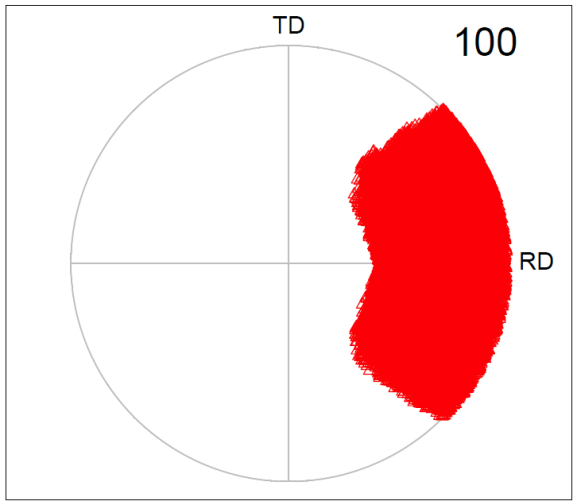

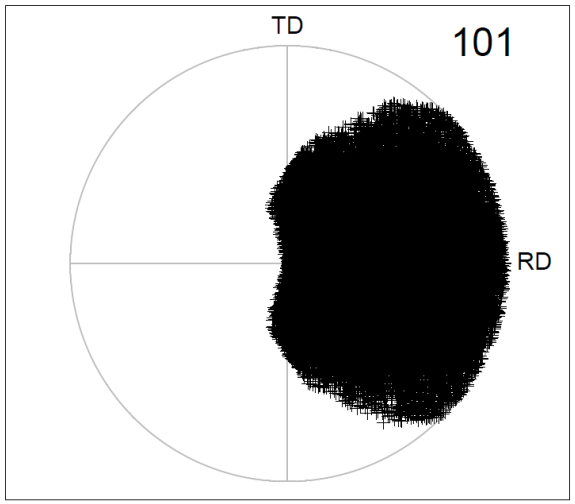

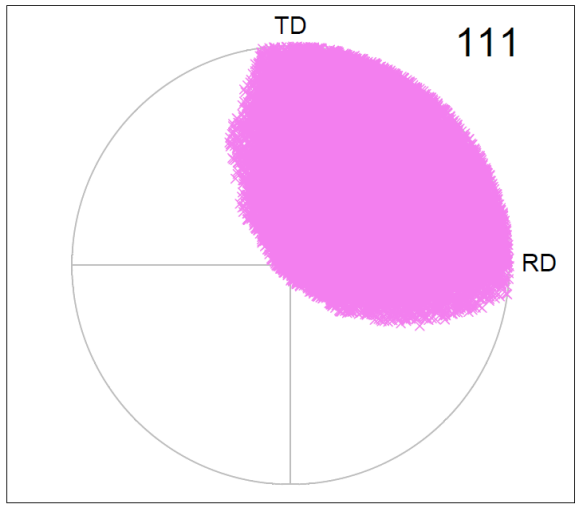

Symmetry application left for the end user!

Orientations pulled from cubic FZ

At the time of production of these slides, the DREAM3D development team has been notified of this error.

ORs and Crystal Symmetry (example)

Inclusion of symmetry in misorientation calculation alleviates the issue of biased “random” orientations from DREAM3D.

Parent Ferrite

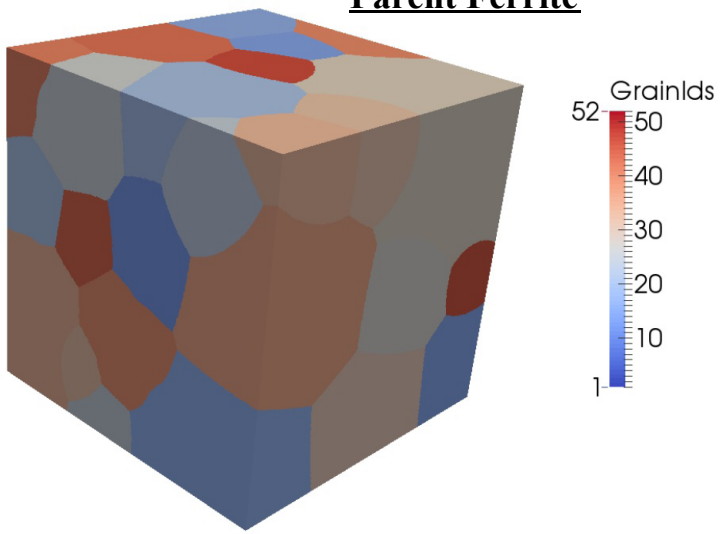

100_B-0_PP

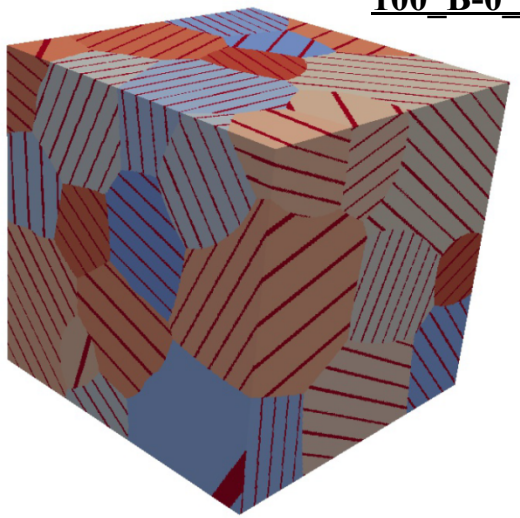

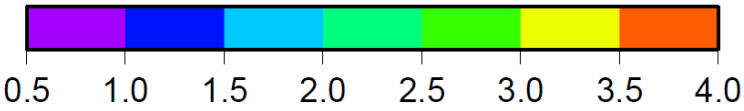

Multiples of Random

No symmetry

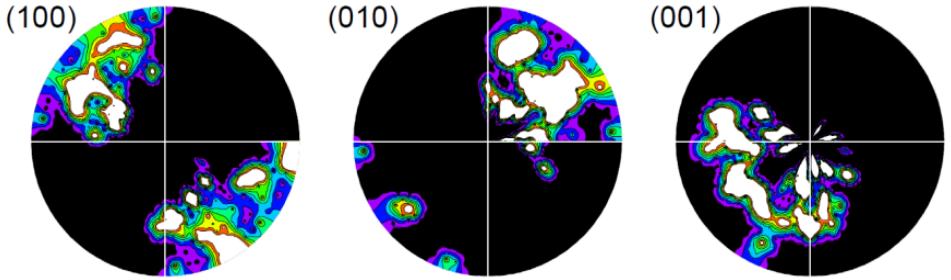

With only BCC symmetry

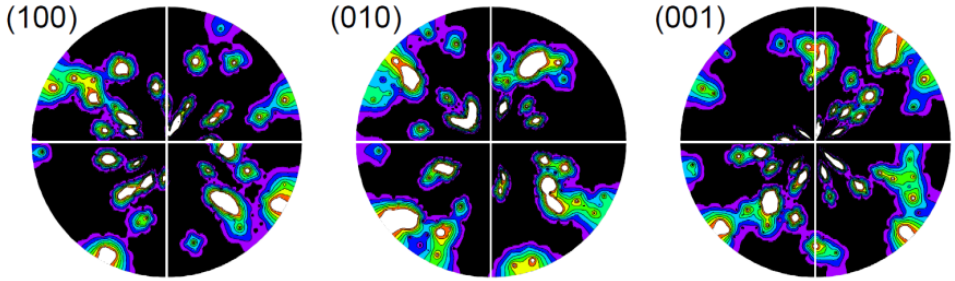

ORs and Crystal Symmetry (example)

Is it necessary to include all symmetry operators?

$$\Delta g = g_\theta g_\alpha^{-1} \rightarrow \Delta g = O_c^\theta g_\theta g_\alpha^{-1} O_c^\alpha$$

Given g_α find g_θ : $O_c^\theta g_\theta = \Delta g \left(g_\alpha^{-1} O_c^\alpha\right)^{-1} \rightarrow g_\theta = \left(O_c^\theta\right)^{-1} \Delta g \left(O_c^\alpha\right)^{-1} \left(g_\alpha^{-1}\right)^{-1}$

$$g_\theta = O_c^\theta \Delta g O_c^\alpha g_\alpha$$

$\Delta g = g_\theta g_\alpha^{-1}$

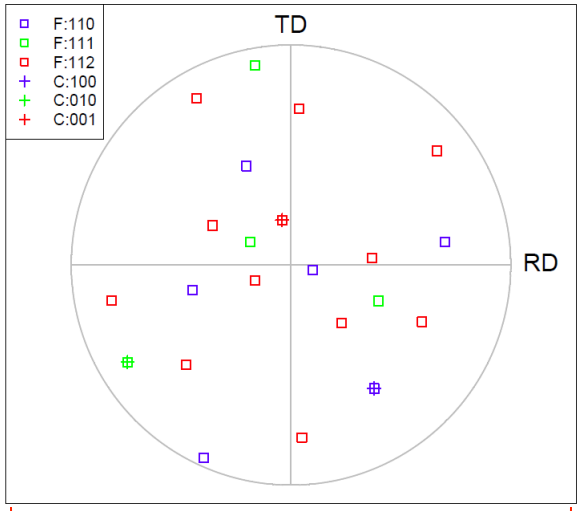

No OR variants

$g_\theta = \Delta g O_c^\alpha g_\alpha$

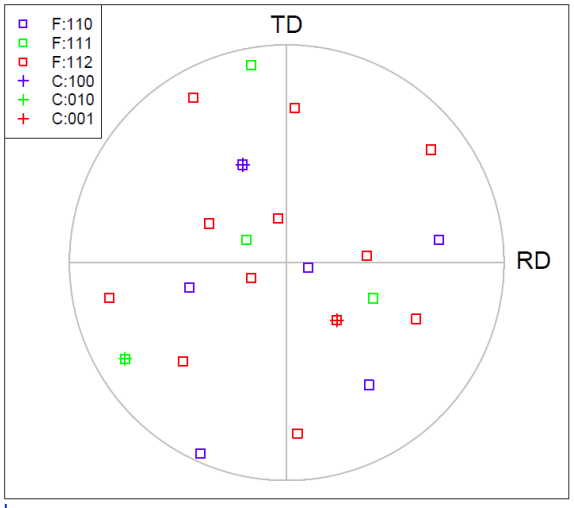

$g_\theta = O_c^\theta \Delta g O_c^\alpha g_\alpha$

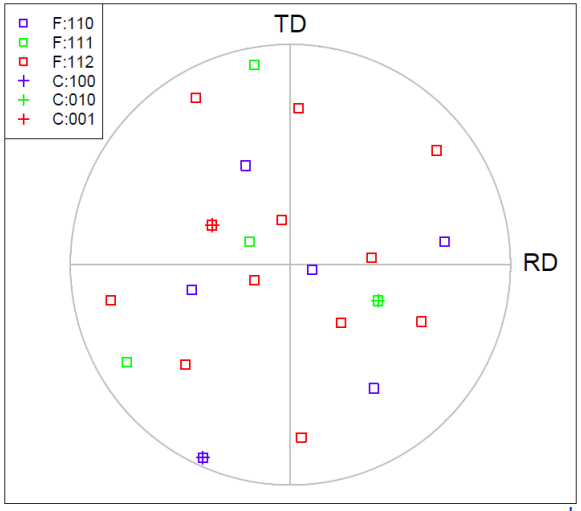

Results in OR variants

OR Variants

Variants of a given OR are specific alignment of planes and directions. These exist because of crystal symmetry

In the K-S OR, there are 4 $\{111\}_\gamma$ planes, each plane parallel to a $\{110\}_\alpha$ plane. A $\{111\}_\gamma$ plane contains 3 $\langle 110\rangle_\gamma$ directions and each $\langle 110\rangle_\gamma$ direction is parallel to 2 $\langle 111\rangle_\alpha$ directions [1]. Hence 24 K-S variants.

$$\begin{bmatrix}1 & 1 & 1\end{bmatrix}_\gamma \parallel \begin{bmatrix}0 & 1 & 1\end{bmatrix}_\alpha$$
$$\begin{bmatrix}\bar{1} & 0 & 1\end{bmatrix}_\gamma \parallel \begin{bmatrix}\bar{1} & \bar{1} & 1\end{bmatrix}_\alpha$$
$$\begin{bmatrix}1 & \bar{2} & 1\end{bmatrix}_\gamma \parallel \begin{bmatrix}2 & \bar{1} & 1\end{bmatrix}_\alpha$$

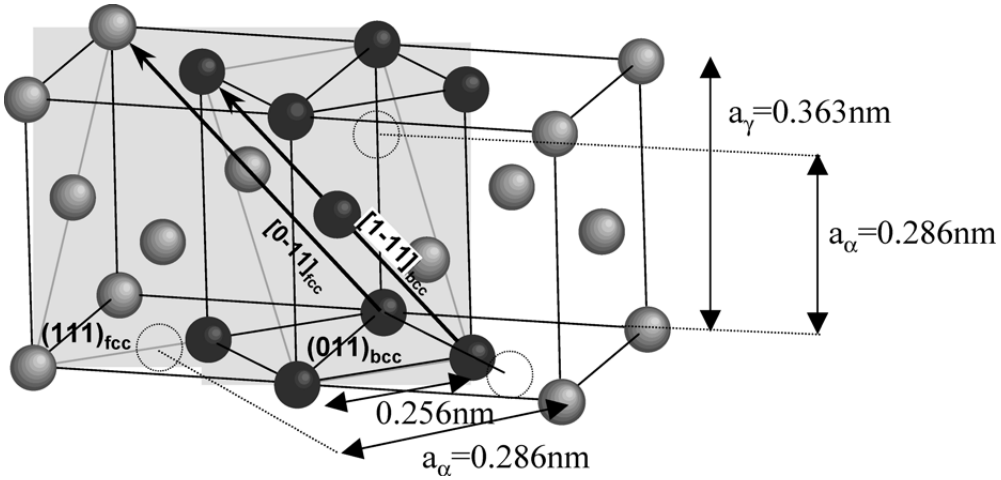

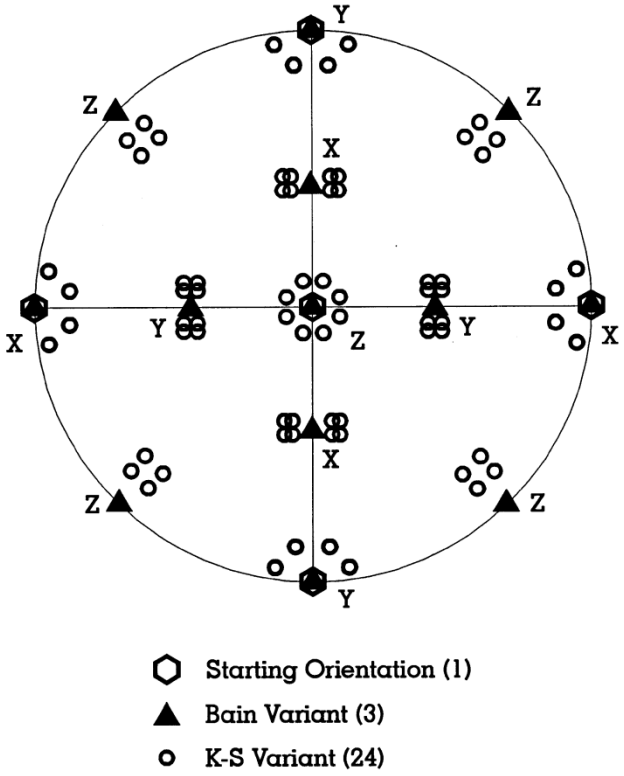

[1] Verbeken, Barbe, Raabe, *ISIJ Int*, 2009 (49) 10, 1601-1609

Butron-Guillen, Da Costa Viana, Jonas, *Met Trans A*, 1997 (28A) 1755-1768

Burgers OR

- Predominant OR observed for body-centered cubic to hexagonal transformation in Ti alloys
- Burgers OR

$(0\ 0\ 0\ 1)_{HCP} \,||\, \{0\ 1\ 1\}_{BCC}$

$[1\ 1\ \text{-}2\ 0]_{HCP} \,||\, \langle 1\ 1\ 1 \rangle_{BCC}$

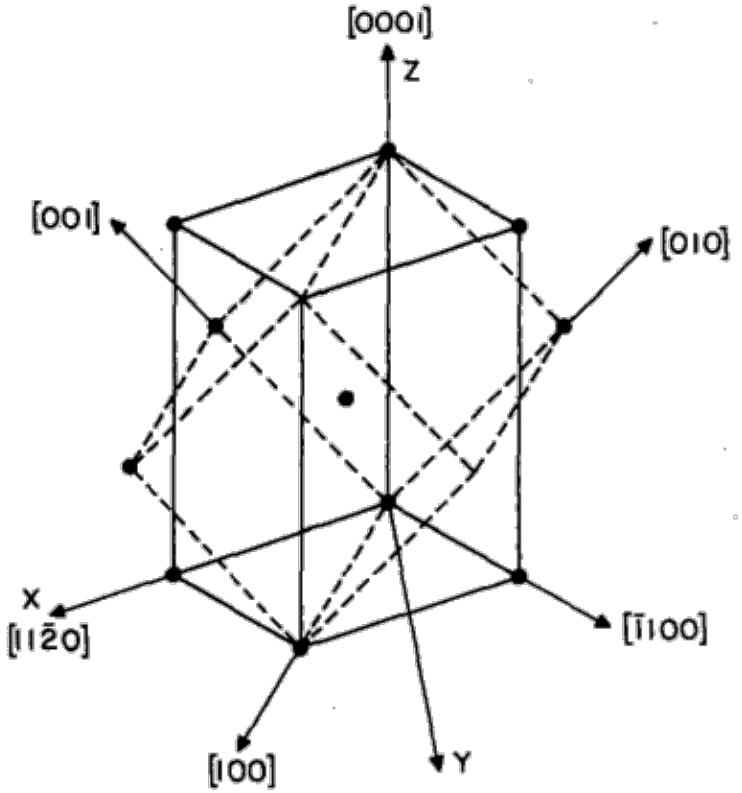

Fig: Geometrical representation of the Burgers OR with dashed lines showing the BCC crystal and continuous lines showing the HCP crystal (Menon et al.,1986)

*Slide courtesy of S Mandal

Burgers OR Variants

- Variants: Each crystallographic orientation relationship predicts different numbers of product orientations originating from a single crystallographic orientation of the parent phase.
- Number of variants is determined by the OR that the product phase have with the parent phase.
- # variants for Burger's OR=12

12 variants of Burgers OR for β to α transformation

Variant number	BCC plane // to $(0001)_\alpha$	BCC direction // to $[11\bar{2}0]_\alpha$
1	(110)	$[\bar{1}1\bar{1}]$
2	(110)	$[1\bar{1}\bar{1}]$
3	$(1\bar{1}0)$	$[11\bar{1}]$
4	$(1\bar{1}0)$	$[111]$
5	(011)	$[11\bar{1}]$
6	(011)	$[\bar{1}1\bar{1}]$
7	$(01\bar{1})$	$[\bar{1}11]$
8	$(01\bar{1})$	$[111]$
9	(101)	$[\bar{1}11]$
10	(101)	$[11\bar{1}]$
11	$(\bar{1}01)$	$[1\bar{1}1]$
12	$(\bar{1}01)$	$[111]$

*Slide courtesy of S Mandal

Variants Selection

- Variants selection: Few of the theoretically predicted variants dominant. Some variants may be preferred over others depending on the transformation mechanism.
- Knowledge about variants selection important to understand microstructure evolution.

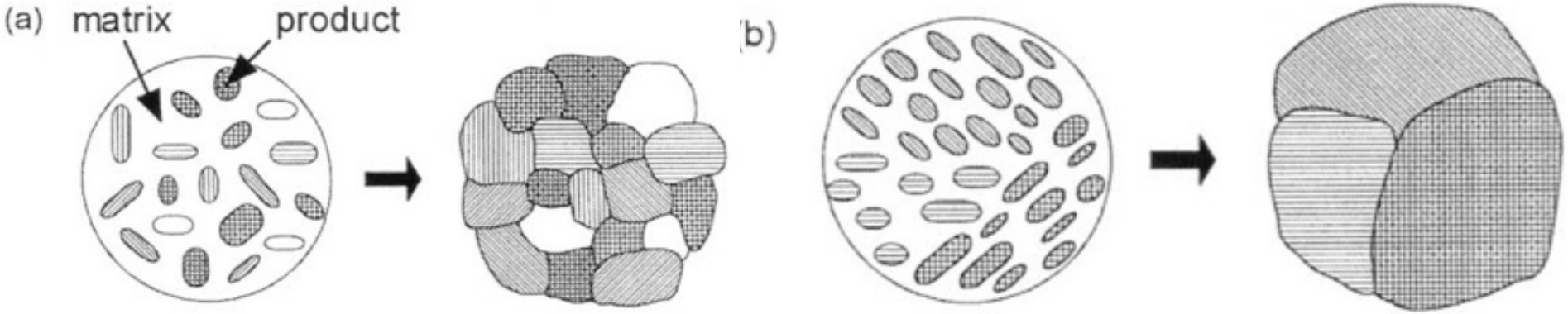

Fig: Evolution of microstructure during diffusional phase transformation (a) without variant selection (each nucleus with a different variant becomes a different grain, resulting in a fine structure). (b) with variant selection (neighboring nuclei having the same variants coalesce to form larger grains). (Furuhara and Maki, 2001)

*Slide courtesy of S Mandal

Stereographic Projection of Burgers OR

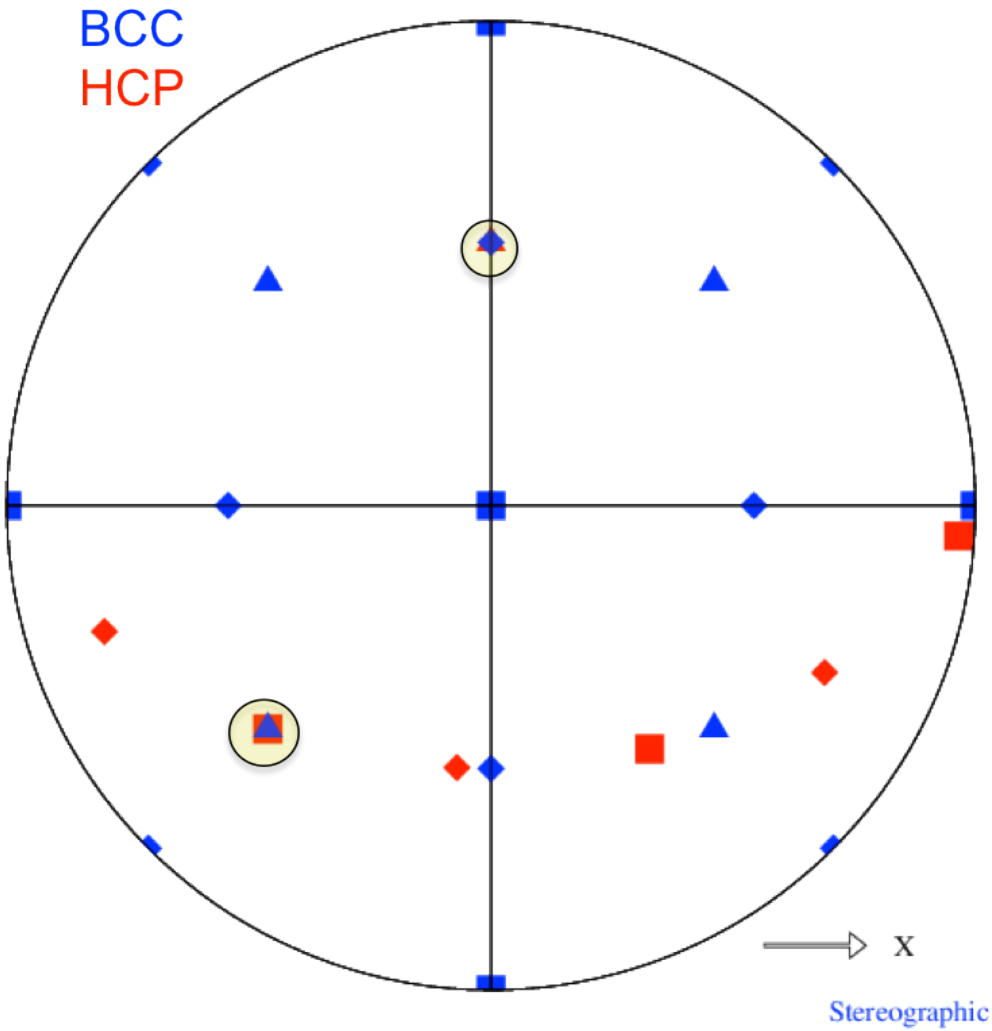

Fig: Stereographic projection for one of the variants of the Burgers OR with a parent BCC orientation of {0,0,0}. Constructed using in-house codes *OR stereogram* and *DrawPF.*

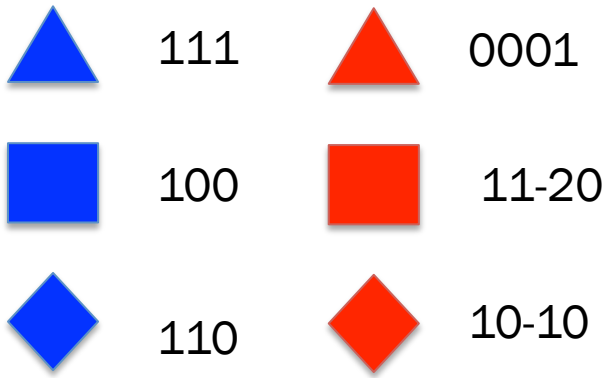

*Slide courtesy of S Mandal

An example

Fig: IPF map of an EBSD dataset. (Provided by IISc)

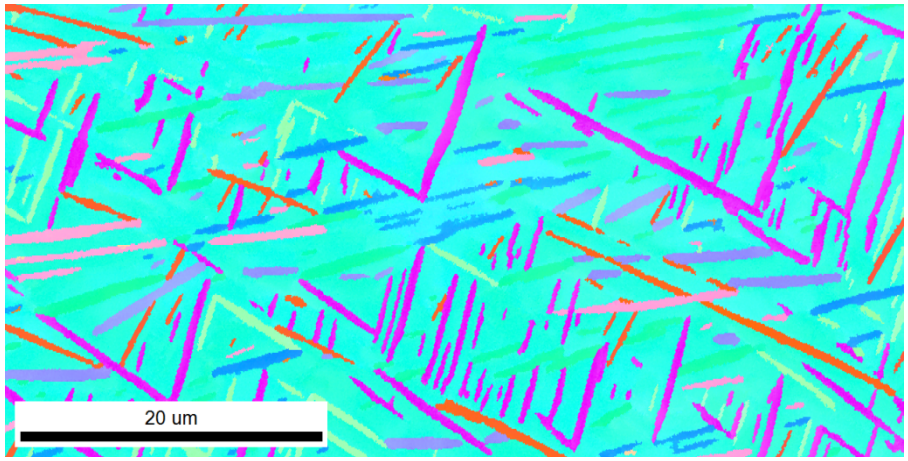

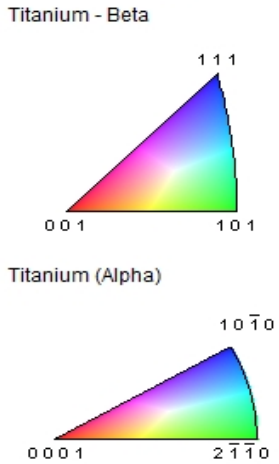

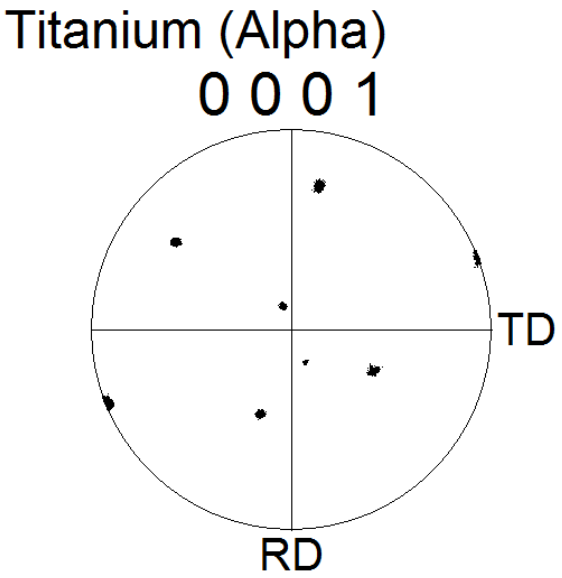

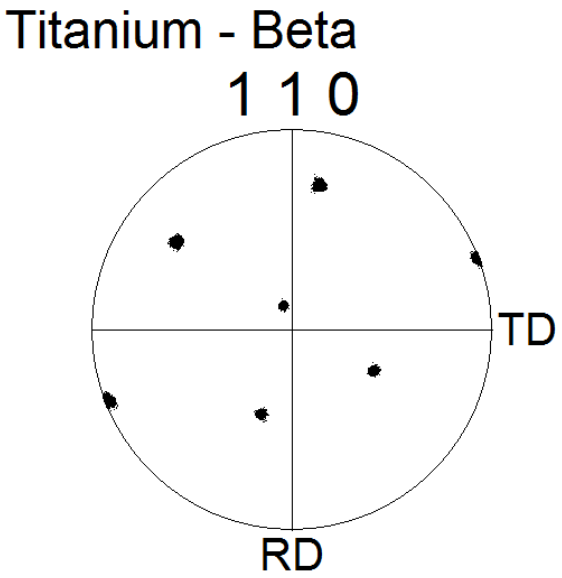

Fig: Pole figures generated using TSL software for this data.

*Slide courtesy of S Mandal

Variants Selection in Ti

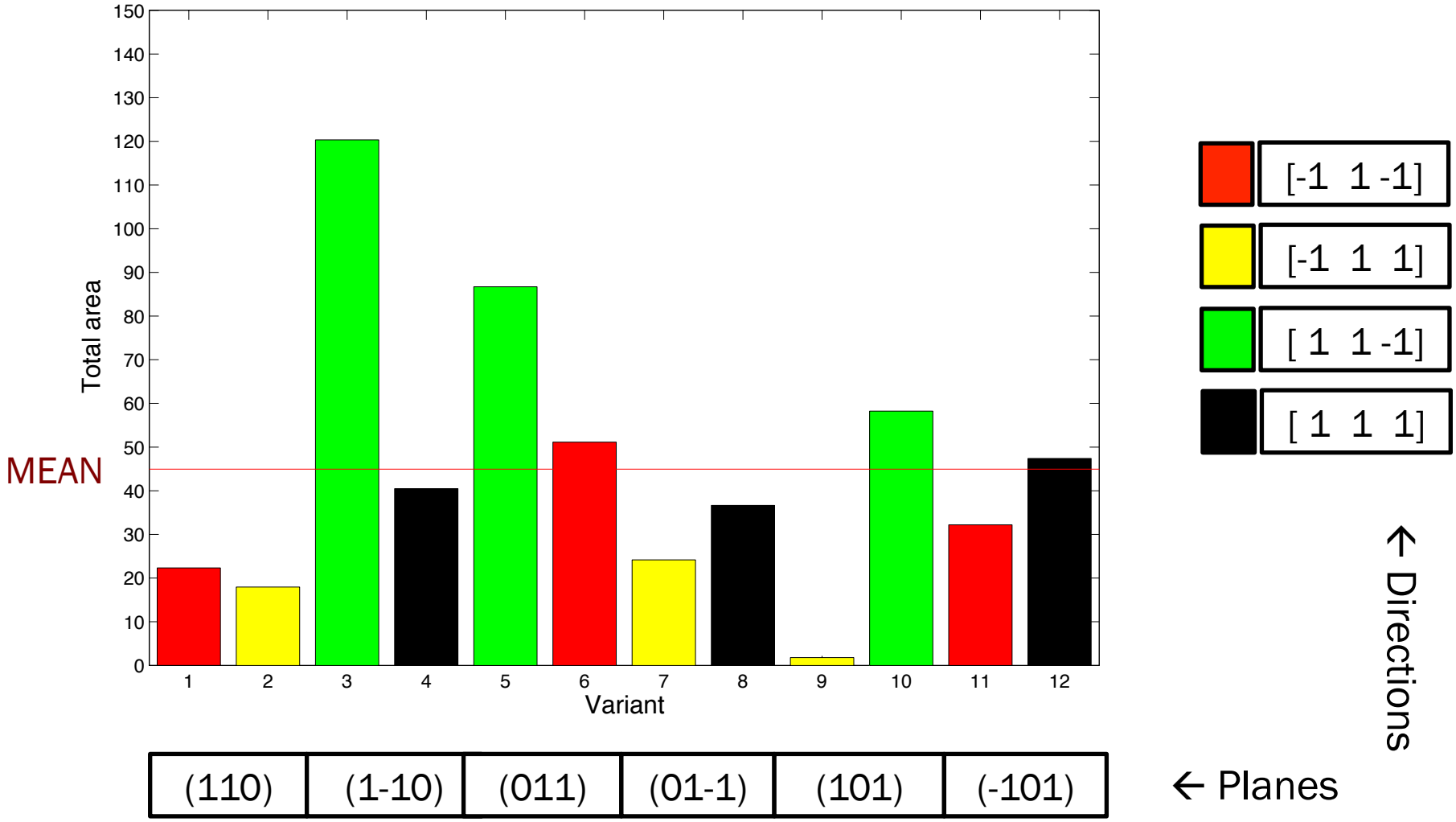

Fig: Relative frequency of variants for the EBSD dataset (Provided by IISC).

*Slide courtesy of S Mandal

Orientation Relationships in Pearlite Microstructures

Pearlite is a lamellar structure comprised of BCC α-ferrite and orthorhombic[1] cementite (Fe3C). A schematic of the pearlitic lamellar structure is shown below, with many different length scales represented: prior austenite grain size, pearlite colony size, interlamellar spacing, and cementite thickness. If a high enough microstructural resolution is used, all length scales should be visible in the vpFFT simulations. This may make a case for the use of multiple SVEs rather than RVEs for this microstructure. (Something to be decided later.) Additionally, because of the sharp and (usually) straight ferrite and cementite interface, there likely exists an orientation relationship (OR) between the two phases. In fact, three ORs have been reported in the literature[2]. Two of these ORs occur with a higher frequency than the third, and these two occur with the same frequency. The three ORs are Bagaryatsky[3], Isaichev[4], and Pitsch-Petch[5,6] and are described on the lower right. The Isaichev OR is the least frequently observed OR.

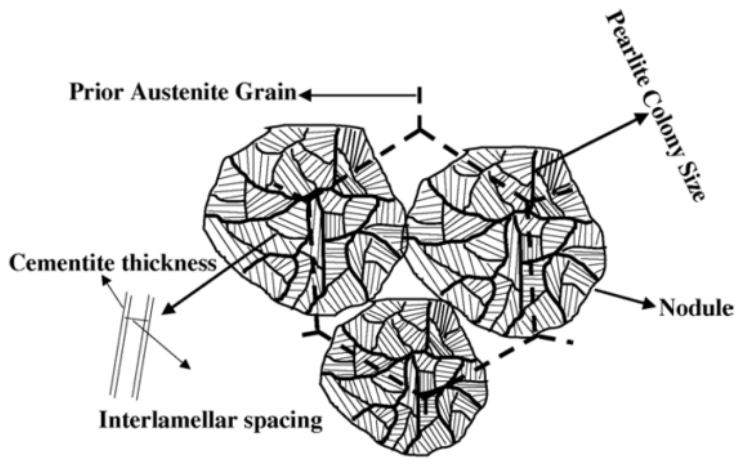

Fig. 1. Schematic diagram illustrating the various constituents in the pearlitic microstructure.

A.M. Elwazri *et al.*,
Mat Sci and Eng A,
404 (2005) 91-98

Bagaryatsky: $[100]c//[1\bar{1}0]f$
$[010]c//[111]f$
$(001)c//(\bar{1}\bar{1}2)f$

Isaichev: $[010]c//[111]f$
$(101)c//(11\bar{2})f$

Pitsch-Petch: $[100]c$ 2.6 deg from $[\bar{3}1\bar{1}]f$
$[010]c$ 2.6 deg from $[131]f$
$(001)c//[21\bar{5}]f$

[1]I.G. Wood *et al.*, J Applied Crystallography, 37 (2004) 82-90
[2]M.A. Mangan, G.J. Shiflet, Met Trans A, 30A (1999) 2767-81
[3]Y.A. Bagaryatsky, Dokl Akad Nauk SSSR, 73 (1950)1161-64
[4]I.V. Isaichev, Z Tekhn Fiz, 17 (1947) 835-38
[5]W. Pitsch, Acta Cryst, 10 (1962) 79-80
[6]N.J. Petch, Acta Cryst, 6 (1953) 96

Further Literature Review of Cementite ORs

Why do different ORs exist for ferrite and cementite in pearlite?

In a large review paper on using electron backscatter diffraction for the study of phase transformations in 2002[1], a section pertaining to pearlite was presented. It cited a 1999 paper[2] which found that the Pitsch-Petch orientation relationship occurs when the pearlite colony nucleates first with cementite. The Bagaryatsky orientation relationship was observed when the pearlite colony nucleated with ferrite. This was observed in both hypereutectoid or hypoeutectoid alloys. All results of ORs were confirmed using EBSD.

A 2009 review paper[3] on predicting orientation relationships using an edge-to-edge matching method to minimize the misfit at an interface stated that using a "selected area electron diffraction" is insufficient resolution to differentiate between the Isaichev and Bagaryatsky ORs. Higher resolution measurements using convergent beam Kikuchi line diffraction patterns never observed the Bagaryatsky OR. They go as far as to say the Pitsch-Petch OR also does not exist, but it is really four distinct ORs which vary less than 6^{o} from Pitsch-Petch. Additionally, the Bagaryatsky and Isaichev OR vary by about 3.5^{o}.

However, in a 2008 PhD thesis[4] the Bagaryatsky OR was observed using EBSD, which has a angular resolution of about 1-2 degrees.

With the small difference between ORs and EBSD confirmation of the Bagaryatsky, I still believe that the Bagaryatsky OR (along with the Pitsch-Petch OR) is still valid and occur about 50/50.

[1]Gourges-Lorenzen, A.F., Int. Materials Reviews, 52 (2002) no. 2
[2]Mangan, Shiflet, Met Trans A, 30A (1999) 2767-2781
[3]Zhang, M.X., Kelly, P.M., Progress in Materials Science, 54 (2009) 1101-1170
[4]Nikolussi, M., PhD Thesis, 2008

Pearlite: Hypothesis and Experiments

Hypothesis: Pearlite colonies containing the Bagaryatsky OR will deform more than those containing the Pitsch-Petch OR.

Concise background relating to hypothesis:

Orientation Relationships

Bagaryatsky: [100]c//[1$\bar{1}$0]f
[010]c//[111]f
Habit Planes → (001)c//($\bar{1}\bar{1}$2)f

Pitsch-Petch: [100]c 2.6 deg from [$\bar{3}$1$\bar{1}$]f
[010]c 2.6 deg from [131]f
Habit Planes → (001)c//[21$\bar{5}$]f

Slip Systems of Pearlite

Ferrite: <111>{110}
<111>{112}

Cementite: <100>{001}
<100>{011}
<111>{110}

Isotropic Elevated Yield Stress

$$\sigma_y = \sigma_0 + k_y S_0^{-1}$$

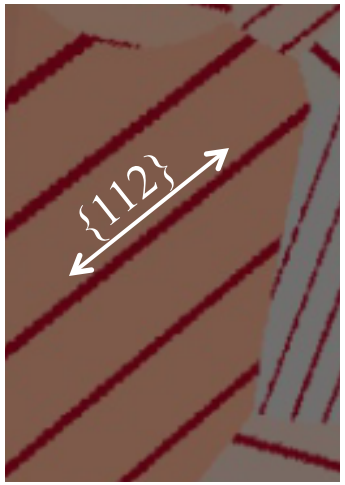

Bagaryatsky OR

With the slip plane in ferrite aligned to the habit plane, long distance between obstacles on this slip plane

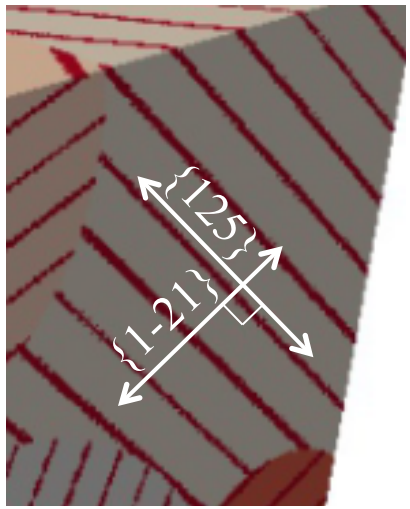

Pitsch-Petch OR

With the slip plane in ferrite misaligned to the habit plane, short distance between obstacles on the {112} slip planes. In fact, {1-21} is perpendicular to {125}

Pearlite: Hypothesis and Experiments

Hypothesis: Pearlite colonies containing the Bagaryatsky OR will deform more than those containing the Pitsch-Petch OR.

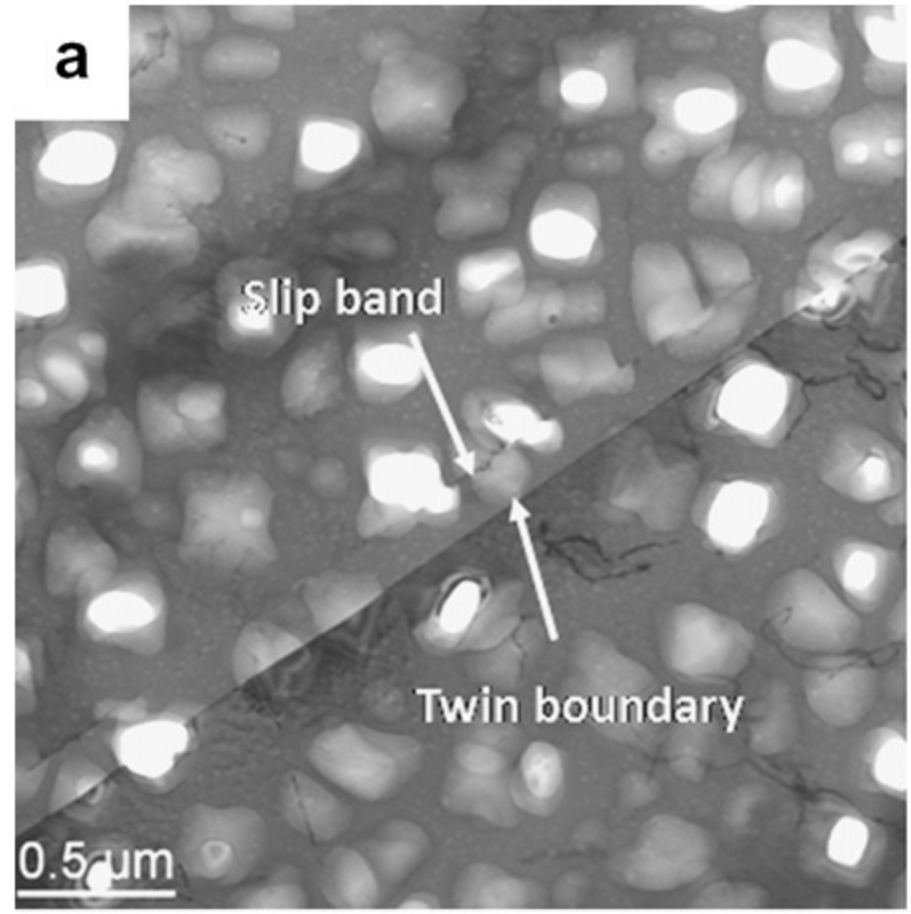

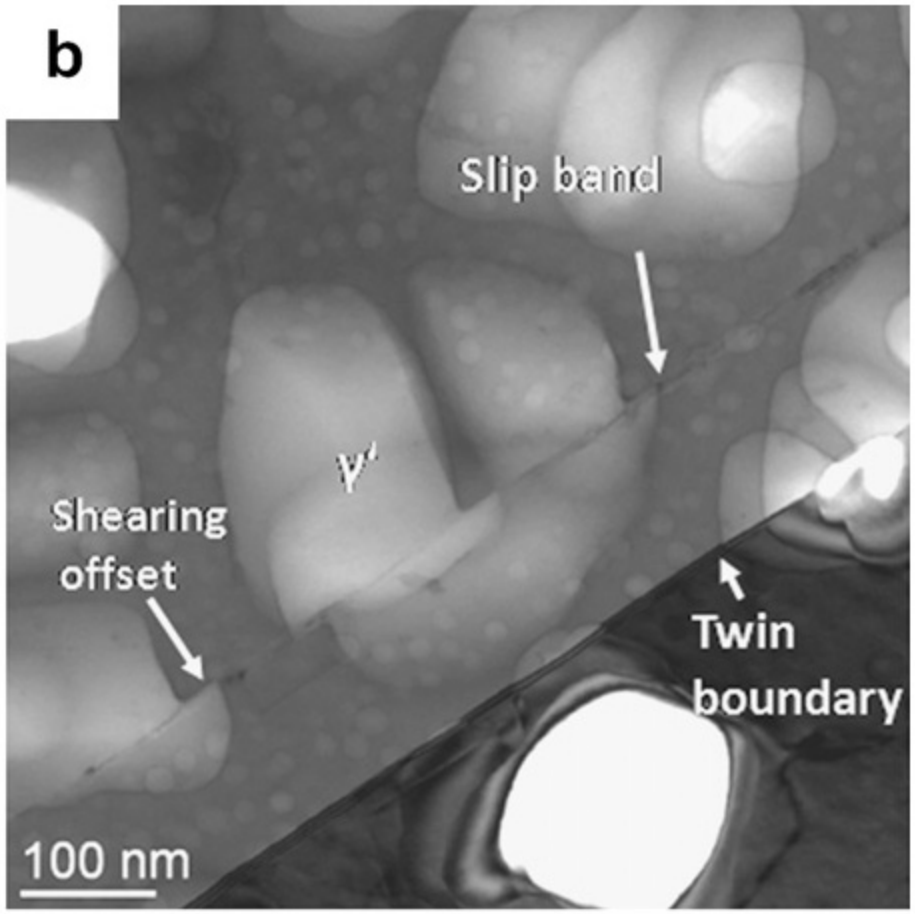

Pearlite: Varying Fractions of the ORs

Testing of this hypothesis is to be performed using the viscoplastic FFT simulations. I am building seven (7) different microstructures from a single parent ferrite grain microstructure. These seven microstructures are:

1.) 0_B-100_PP – 100% of all parent ferrite grains spawn cementite lamellae with the Pitsch-Petch OR
2.) 25_B-75_PP – 75% of all parent ferrite grains spawn cementite lamellae with the Pitsch-Petch OR, the other 25% of all parent ferrite grains spawn cementite lamellae with the Bagaryatsky OR
3.) 50_B-50_PP – 50% of all parent ferrite grains spawn cementite lamellae with the Pitsch-Petch OR, the other 50% of all parent ferrite grains spawn cementite lamellae with the Bagaryatsky OR
4.) 75_B-25_PP – 25% of all parent ferrite grains spawn cementite lamellae with the Pitsch-Petch OR, the other 75% of all parent ferrite grains spawn cementite lamellae with the Bagaryatsky OR
5.) 100_B-0_PP – 100% of all parent ferrite grains spawn cementite lamellae with the Bagaryatsky OR
6.) Polycrystalline – this microstructure is the parent ferrite grains with a number of ferrite grains switched phase switched to cementite (from ferrite) to match the 16% volume fraction of cementite in pearlite
7.) Ferrite only – this microstructure is simply the parent ferrite grains

Recall that there is no true length scale involved in the FFT simulations. So the simulations are not informed as to the length to the nearest boundary which will impede slip on a given slip system. That is to say, these tests will simply test if the introduction of different ORs in the microstructure play a role in the deformation behavior of pearlite. Additionally, comparison of the lamellar microstructure to the polycrystalline sample accentuates the role of the different ORs compared to a simple incorporation of cementite in to the system.

ORs are assigned in the order in which the parent grains are randomly selected making the assignment of OR to each grain random. Additionally, the axis along which the OR is place (the (-1-12) in the case of Bagaryatsky) is also done with a random symmetry operator (belonging to the cubic set).

while inserted_twins < desired_number_of_twins AND unfilled_grains?

  Randomly select grainID

  Get grain orientation g_i

  while room for twin within grainID

    What is the habit plane normal, v_c, in crystal reference frame?

    Choose random crystal symmetry operator for crystal class of
      parent grain $O_c^{(n)}$

    Apply crystal symmetry $v_c' = O_c^{(n)} v_c$

    Find direction in sample space $v_s = g_1^T v_c'$

    Construct grain geometry of twin/lamella within parent grain

    Define rotation from parent orientation to twin/lamella
      orientation, Δg, by orientation relationship

    Assign lamella twin/orientation g_t by
      $g_t = \Delta g \; O_c^{(n)} g_i$

    More twins to insert within grain?

  done

  All grains filled with twins?

  More twins to insert overall?

done

Pearlite: Varying Fractions of the ORs
Grain Structure Images

Ferrite Only

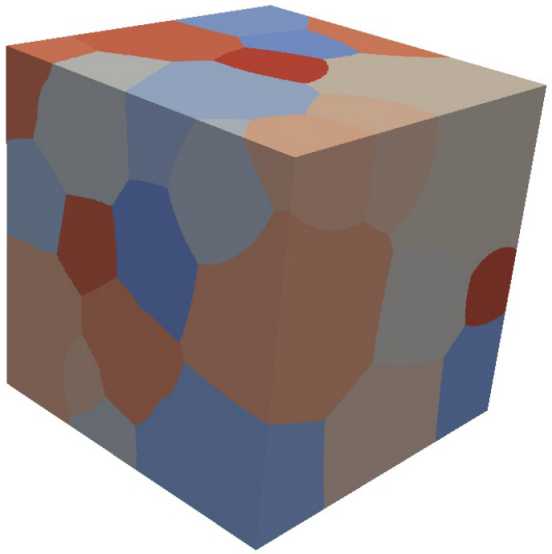

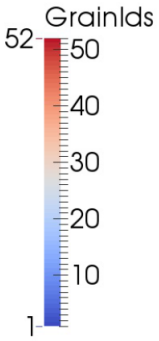

Polycrystalline

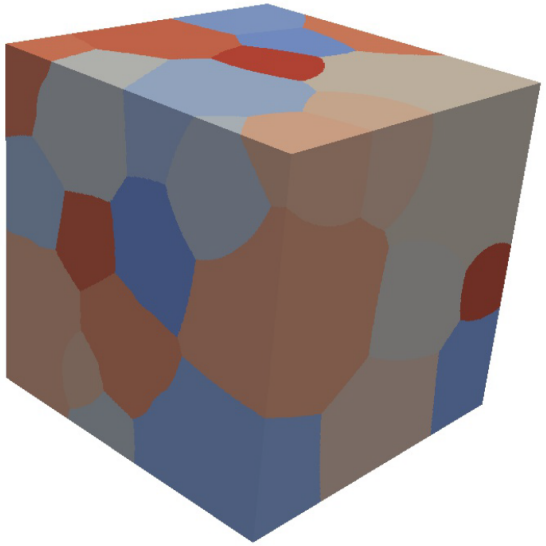

Colored by grain number

Polycrystalline – Distribution of Cementite Phase

Colored by phase – red = cementite

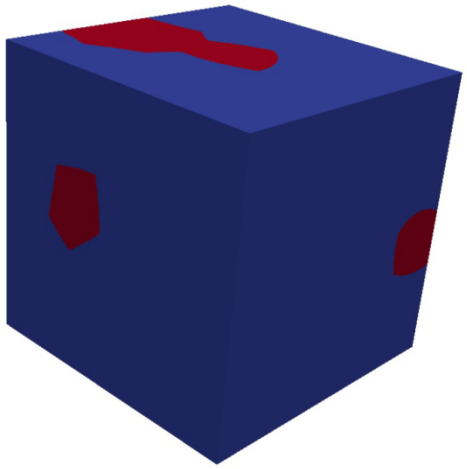

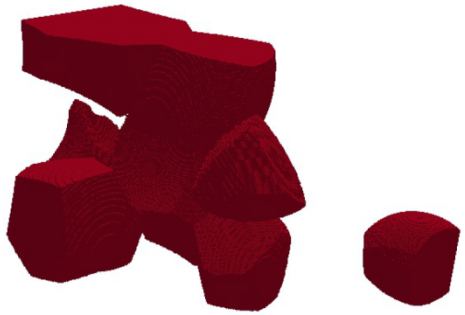

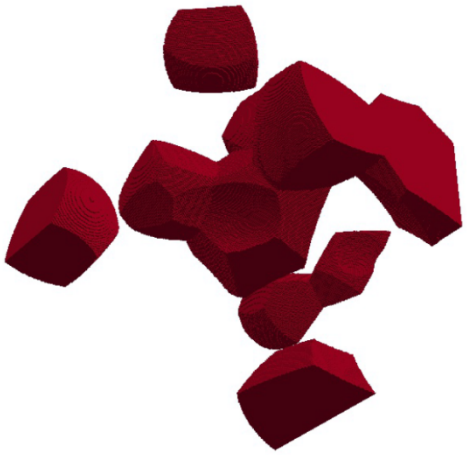

Pearlite: Varying Fractions of the ORs Grain Structure Images (Cont'd)

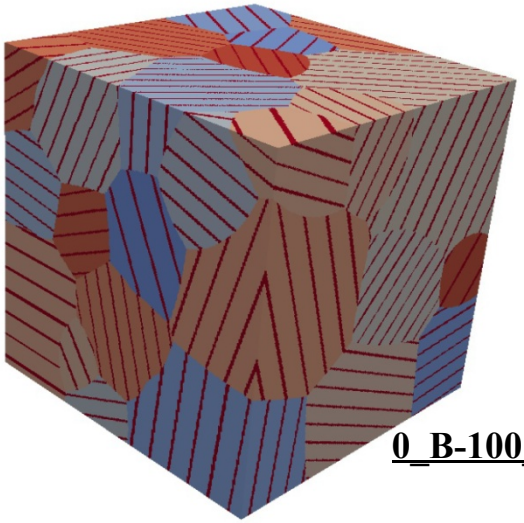

0_B-100_PP

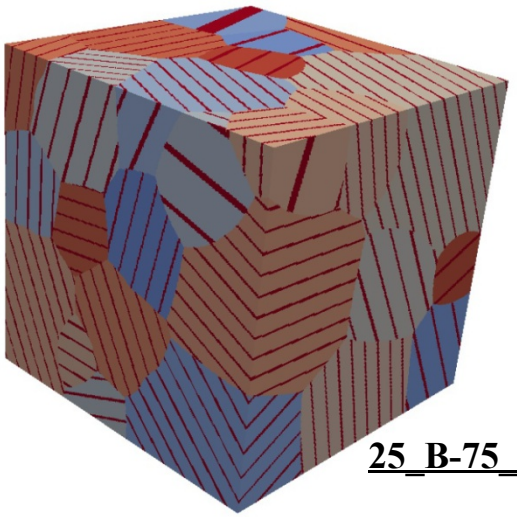

25_B-75_PP

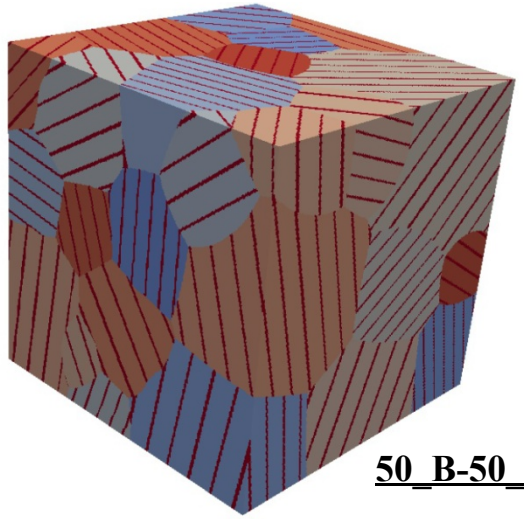

50_B-50_PP

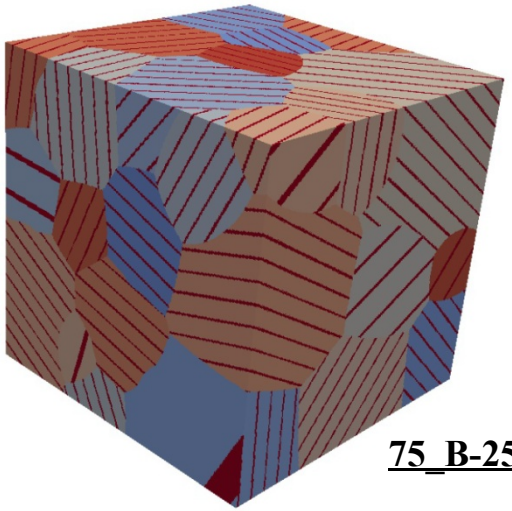

75_B-25_PP

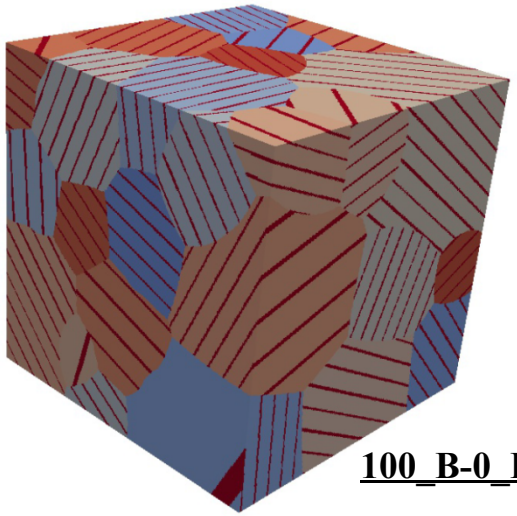

100_B-0_PP

Colored by grain number
dark red = cementite grains

Pearlite: Varying Fractions of the ORs Grain Structures

Recall that the Fe-C equilibrium phase diagram predicts the weight fraction of cementite be about 11%. The table on the right displays the measured volume fraction (for simplicity, assumed to be equivalent to weight fraction) of the cementite in each microstructure.

The number of twins inserted in to the 51 parent ferrite grains are also listed.

Structure	Vol. Frac. Cementite	No. of Twins Inserted
0_B-100_PP	0.124	381
25_B-75_PP	0.126	378
50_B-50_PP	0.123	373
75_B-25_PP	0.125	377
100_B-0_PP	0.124	380
Polycrystalline	0.125	0
Ferrite Only	0.000	0
Fe-C Equilibrium Phase Diagram	0.1105	——

0_B-100_PP **25_B-75_PP** **50_B-50_PP** **75_B-25_PP** **100_B-0_PP** **Ferrite Only** **Polycrystalline**

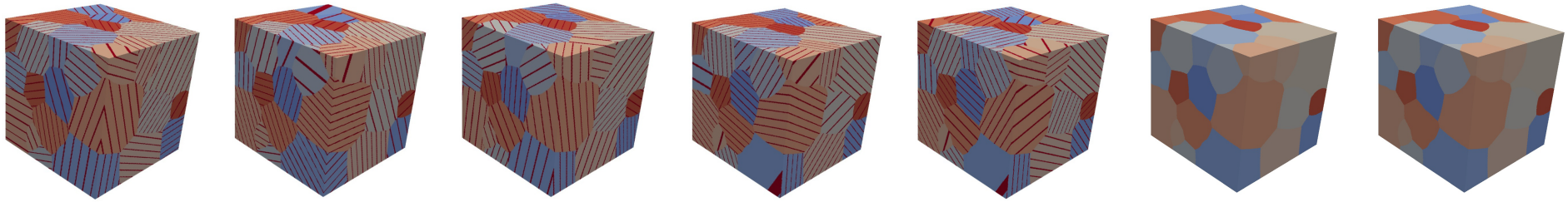

Pearlite: Varying Fractions of the ORs Stress Strain Curves

These are the overall stress-strain curves for the tested microstructures. The variation in stress response in the pearlitic microstructures no longer increases with increasing Pitsch-Petch orientation relationship.

Notice the lowest stresses are found in microstructures without cementite. Introduction of cementite just as a second phase (polycrystalline) only slightly increases by 200 MPa.

The restriction of cementite to a lamellar structure additionally increases stress values. On average, this is an increase of 350 MPa for the 100_B-0_PP microstructure.

The average difference between the 100_B-0_PP and 25_B-75_PP curves is 80 MPa.

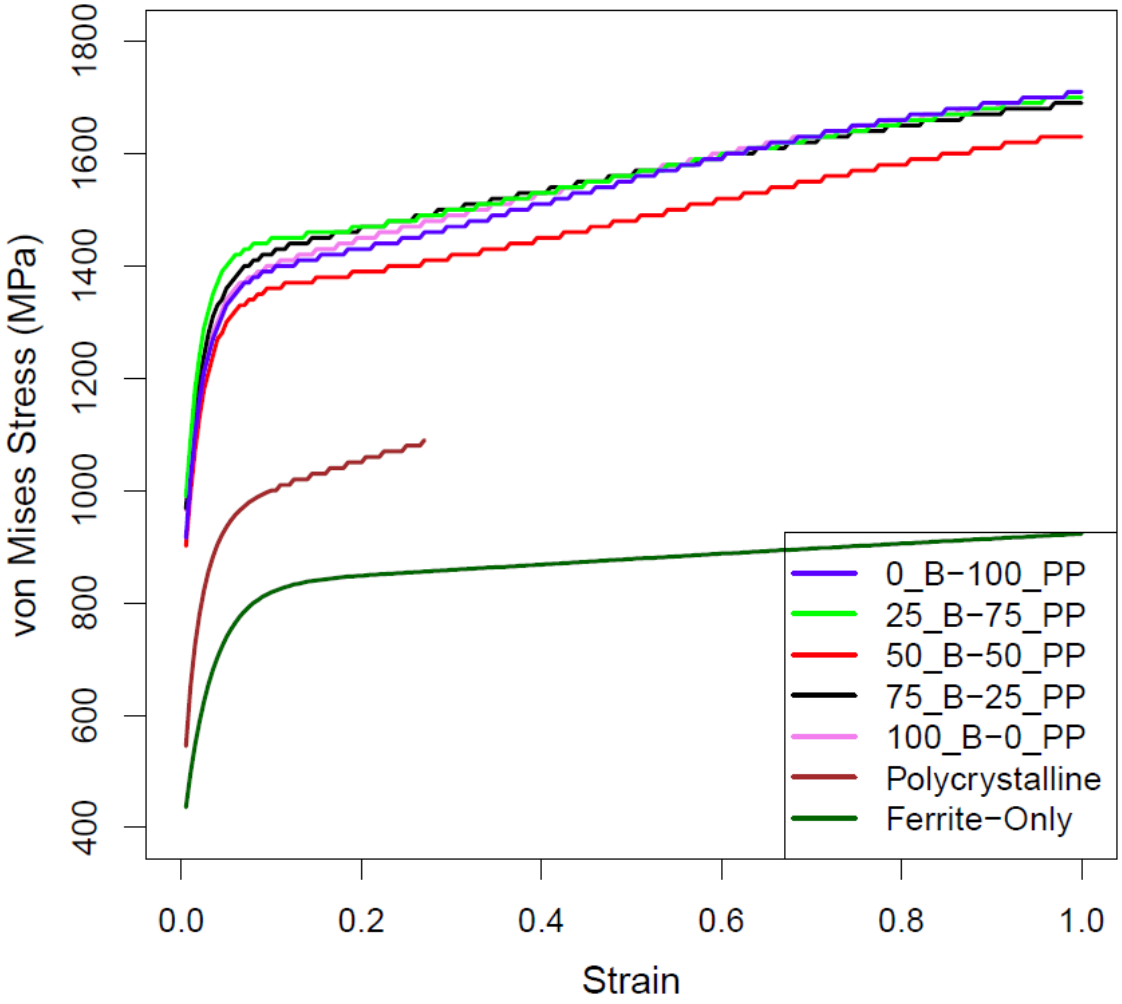

Pearlite: Varying Fractions of the ORs Stress Strain Curves

To test the likelihood of the orientation playing a dominating role on the deformation behavior, I took the original 50_B-50_PP grain structure and assigned orientations to all grains at random. I did this 10 times.

The results to the right show the range of stress response possible for various orientations given this grain structure. The average difference between the highest and lowest stress-strain curves is ~40 MPa.

Therefore, it seems reasonable that some differences in response for the microstructures is due to the structure itself. (i.e. the spatial orientations of the lamellae, which is somewhat controlled by the parent ferrite orientation)

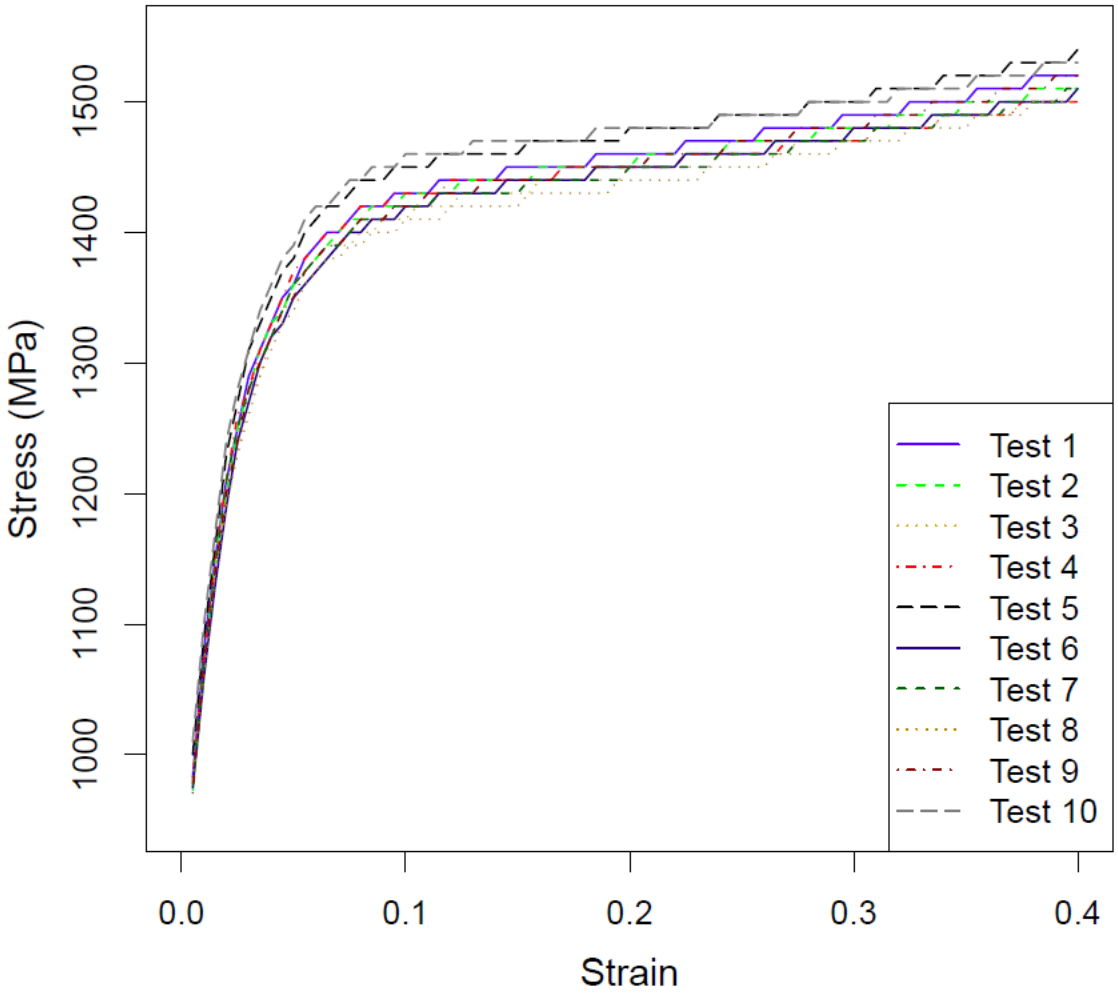

Texture Development
0% Strain – Cementite

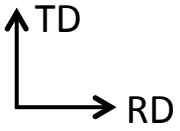

0_B-100_PP

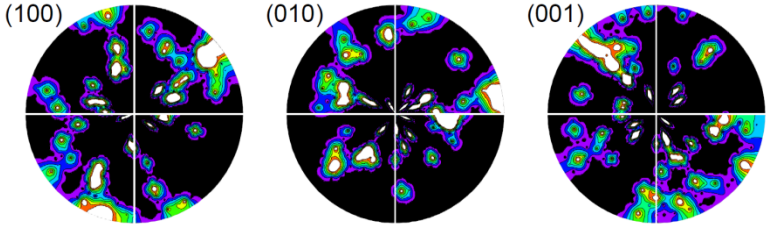

25_B-75_PP

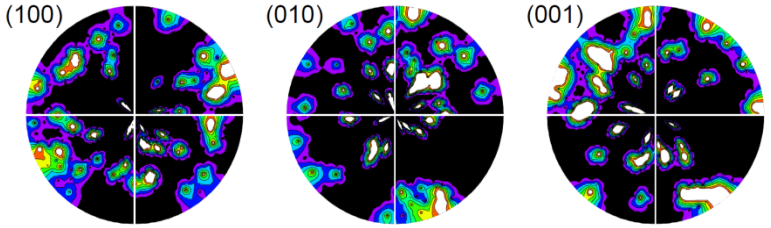

50_B-50_PP

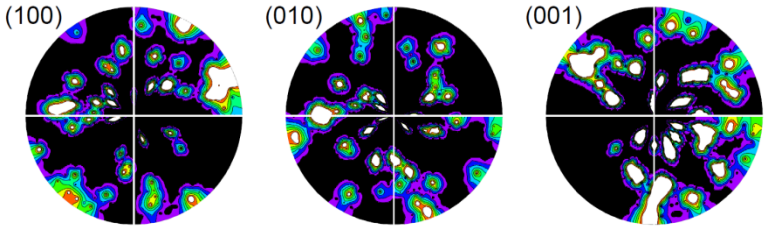

75_B-25_PP

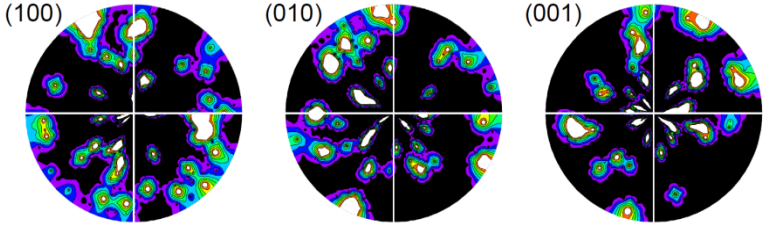

100_B-0_PP

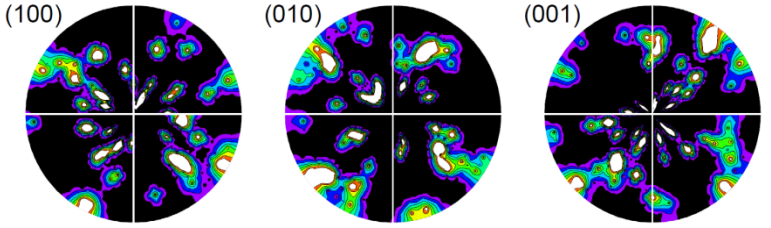

Texture Development
100% Strain – Cementite

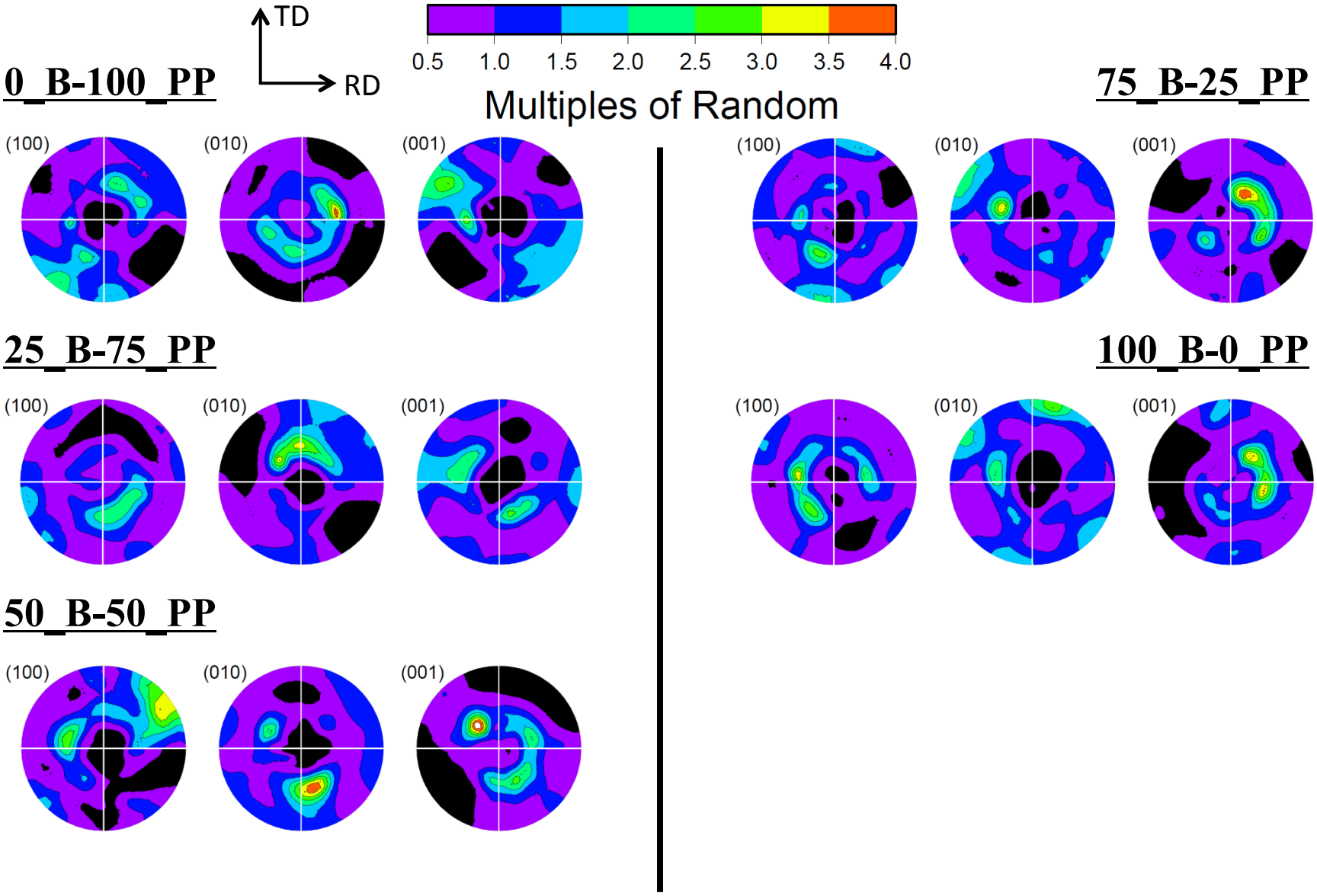

Texture Development
100% Strain – Ferrite

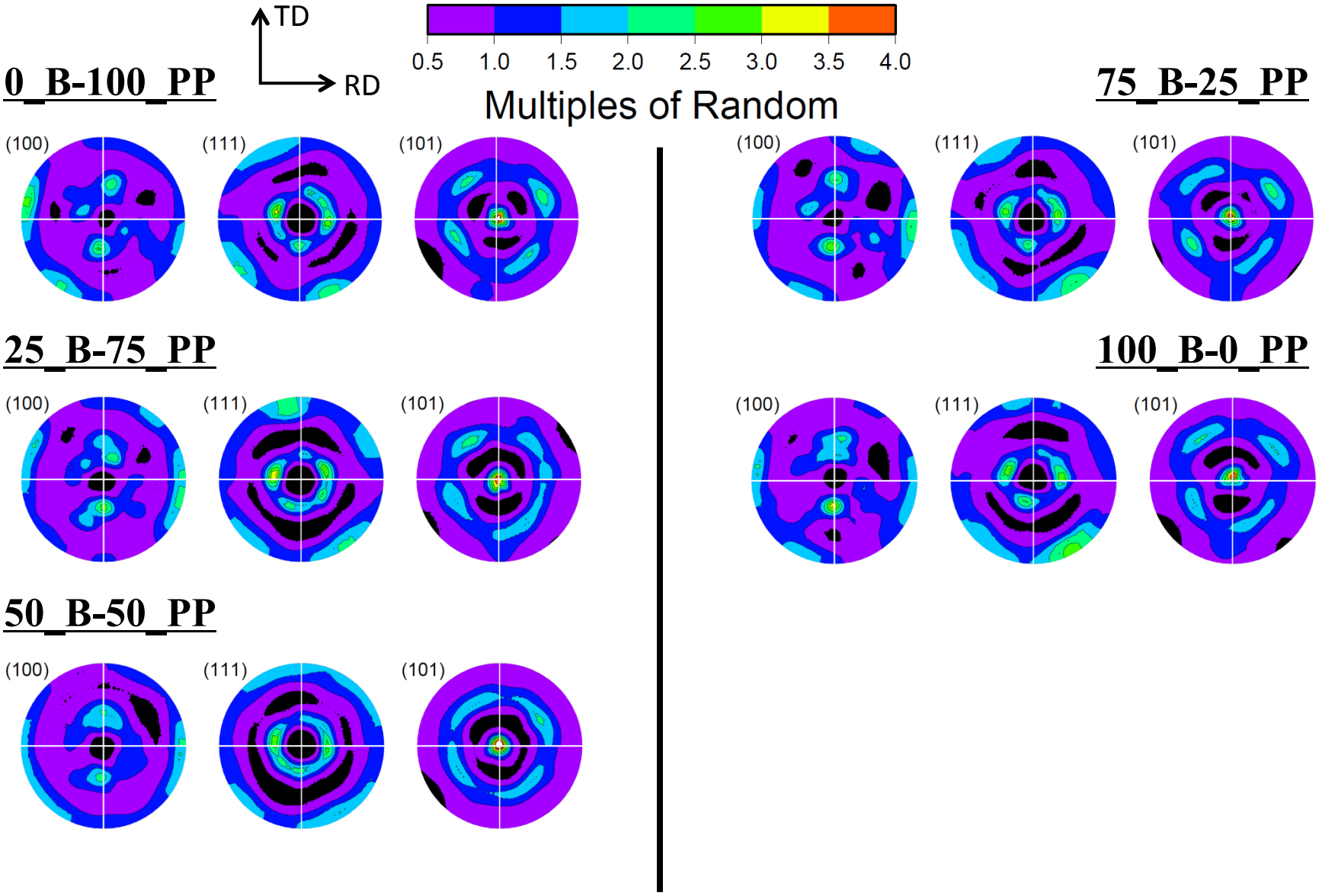

Partitioning by OR
Non-random ferrite orientations

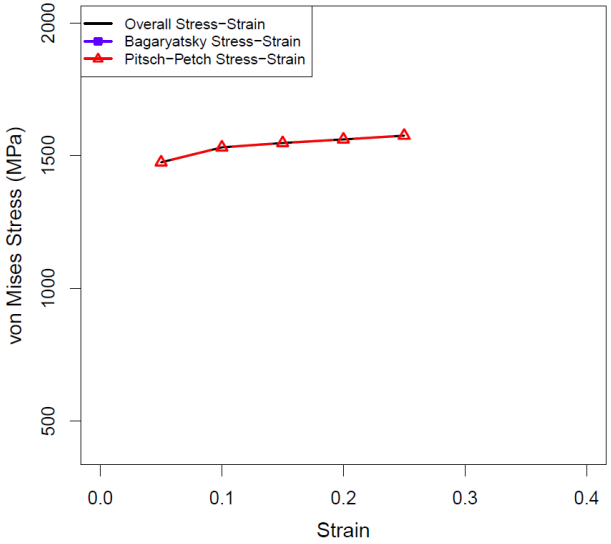

0_B-100_PP

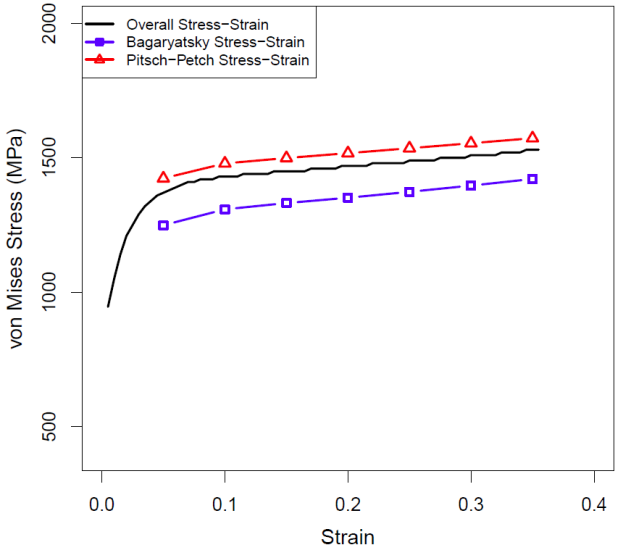

25_B-75_PP

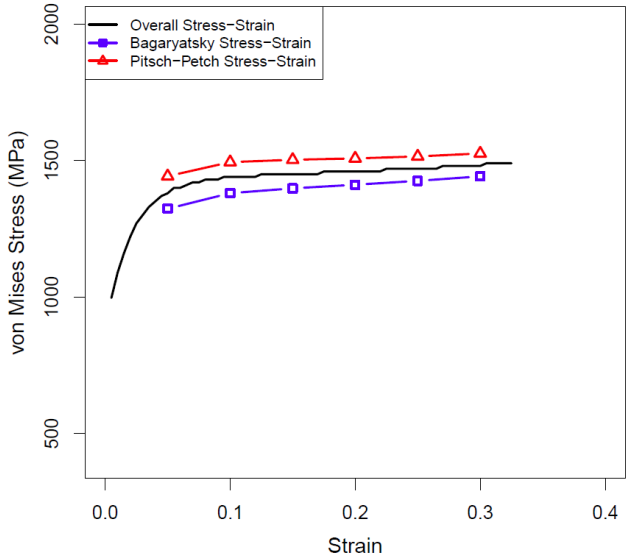

50_B-50_PP

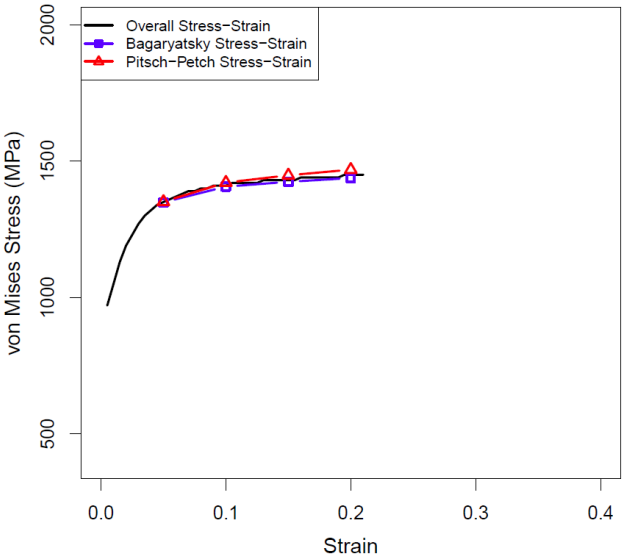

75_B-25_PP

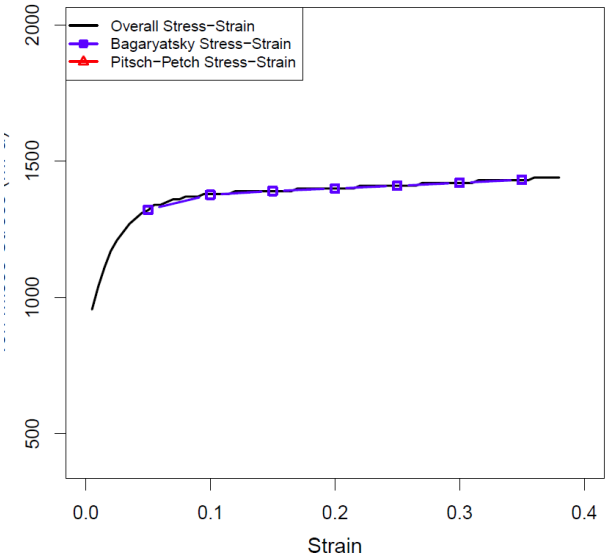

100_B-0_PP

No matter the fraction of the OR present, grains (ferrite and cementite) associated with the Pitsch-Petch OR contain a higher stress value on average than those associated with the Bagaryatsky. This agrees with the hypothesis.

For 0_B-100_PP and 100_B-0_PP the partitioned values match the overall curve (obviously).

Partitioning by Phase
Non-random ferrite orientations

Ferrite

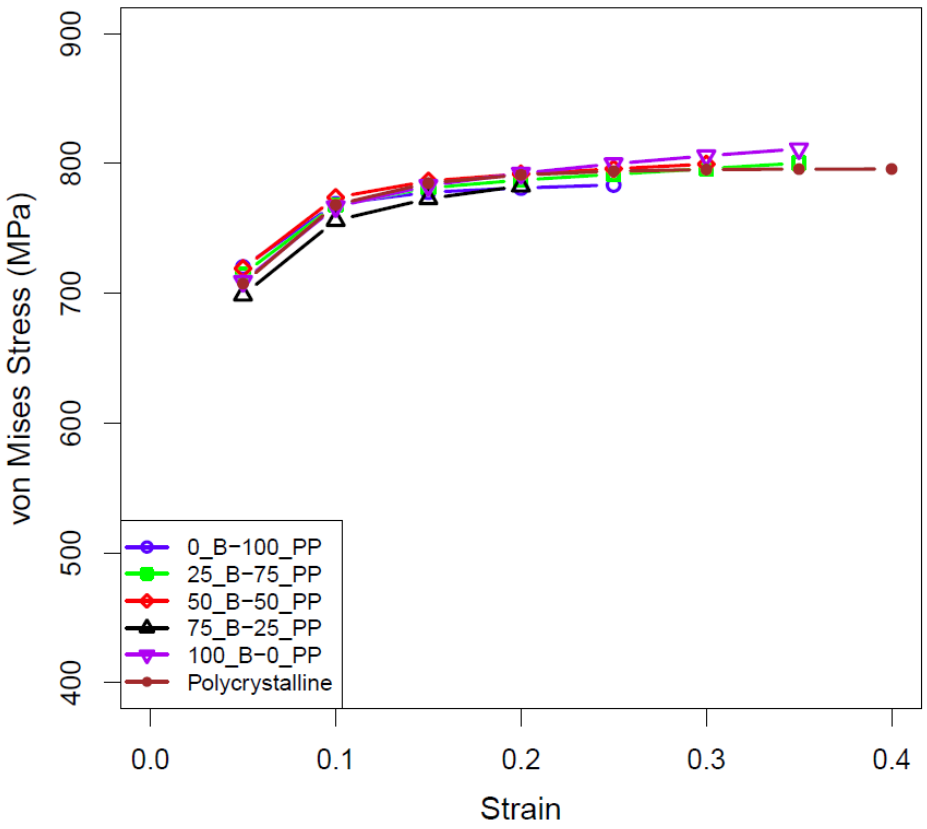

Cementite

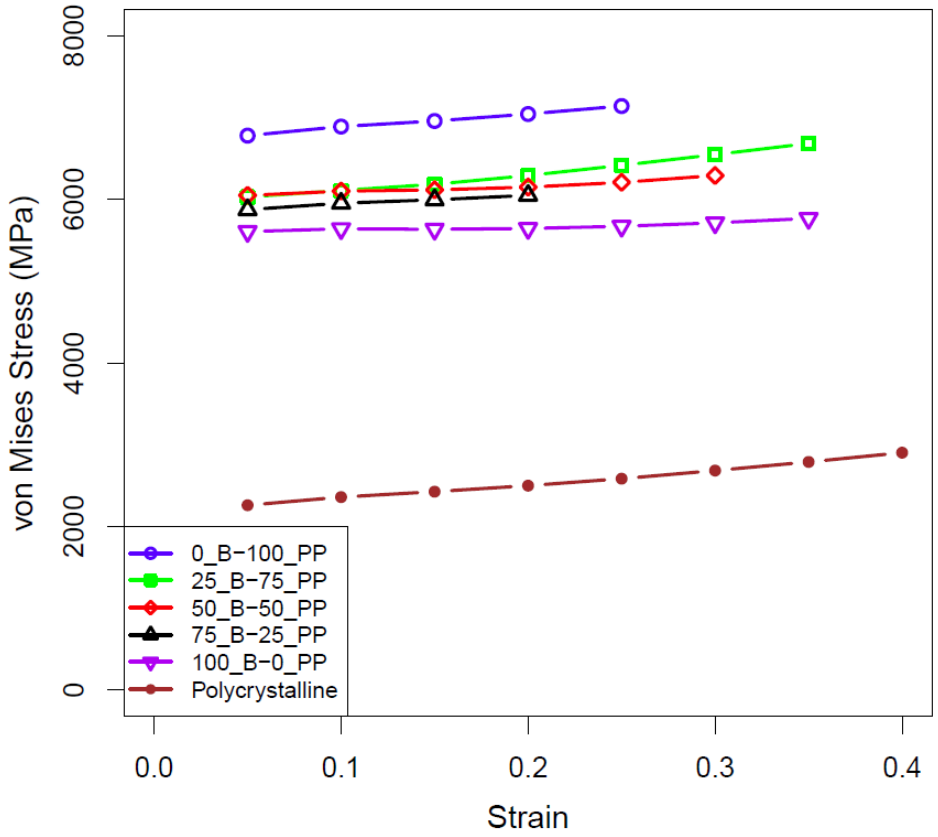

It is interesting to see that regardless of the OR fraction, the stress values in ferrite do not vary much. However, the cementite stress values seem quite dependent on the OR. While the overall response of the pearlite agrees with the hypothesis, my reasoning seems wrong. I reasoned that in the Bagaryatsky OR the ferrite slip-plane is highly aligned with the interface plane allowing for dislocations to move longer distances prior to encounter obstacles. Currently, I do not have reasoning as to why cementite, instead of ferrite, is sensitive to the OR.

Microstructure of Martensite

- The microstructural characteristics of martensite are:
  - the product (martensite) phase has a well defined crystallographic relationship with the parent (matrix).
  - martensite forms as platelets within grains.
  - each platelet is accompanied by a shape change
  - the shape change appears to be a simple shear parallel to a habit plane (the common, coherent plane between the phases) and a uniaxial expansion (dilatation) normal to the habit plane. The habit plane in plain-carbon steels is close to {225}, for example (see P&E fig. 6.11).
  - successive sets of platelets form, each generation forming between pairs of the previous set.
  - the transformation rarely goes to completion.

*Slide courtesy of AD Rollett

Microstructures

Martensite formation rarely goes to completion because of the strain associated with the product that leads to back stresses in the parent phase.

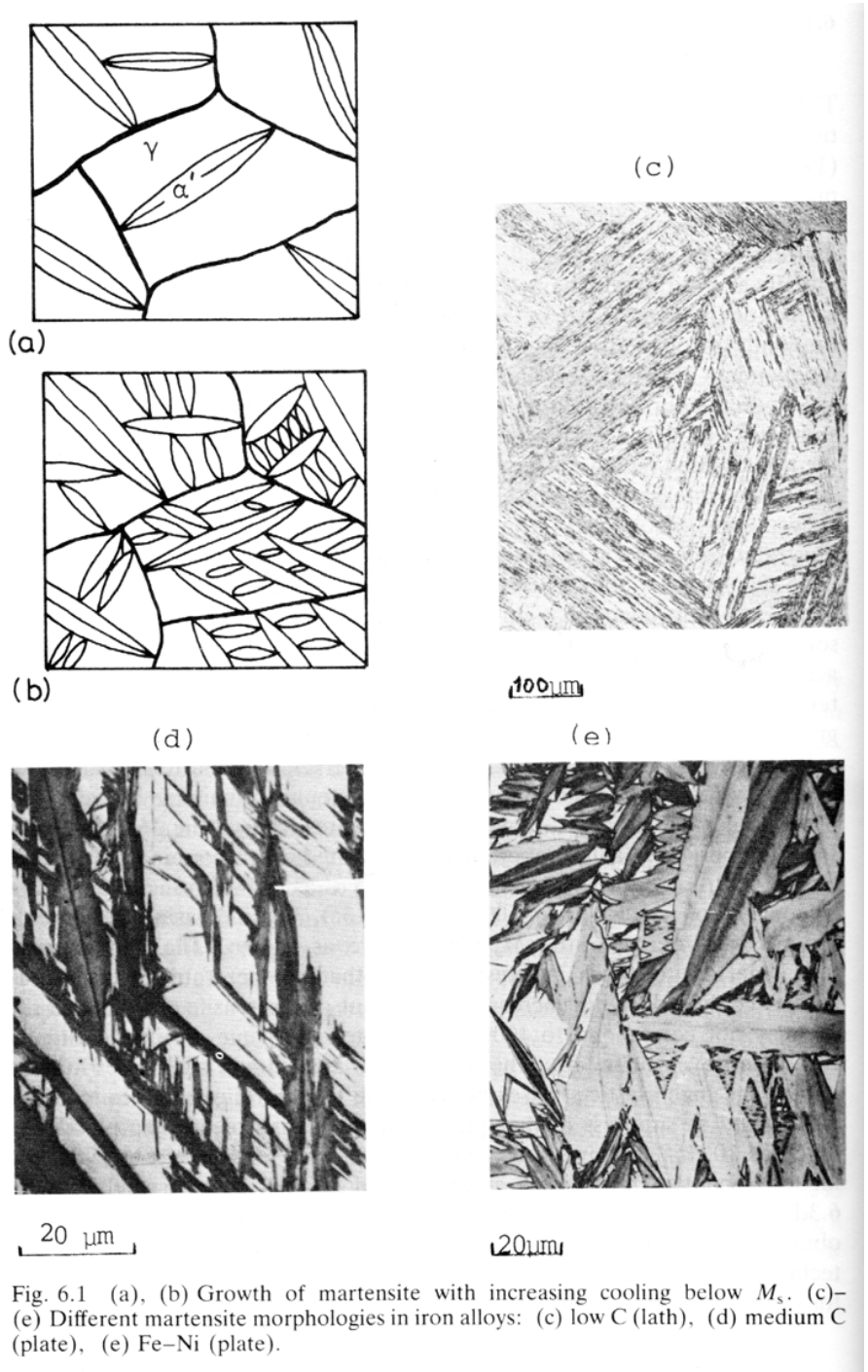

Fig. 6.1 (a), (b) Growth of martensite with increasing cooling below M_s. (c)–(e) Different martensite morphologies in iron alloys: (c) low C (lath), (d) medium C (plate), (e) Fe–Ni (plate).

*Slide courtesy of AD Rollett

Shear strain in martensite formation

- The change in shape that occurs during martensite formation is important to understanding its morphology.
- In most cases there is a large shear strain. This shear strain is, however, opposed by the surrounding material.
- A typical feature of martensitic transformations is that each colony of martensite laths/plates consists of a stack in which different variants alternate. This allows large shears to be accommodated with minimal macroscopic shear. The reason for this morphology is that the volume of matrix affected by the sheared material is minimized by this alternating pattern of laths.

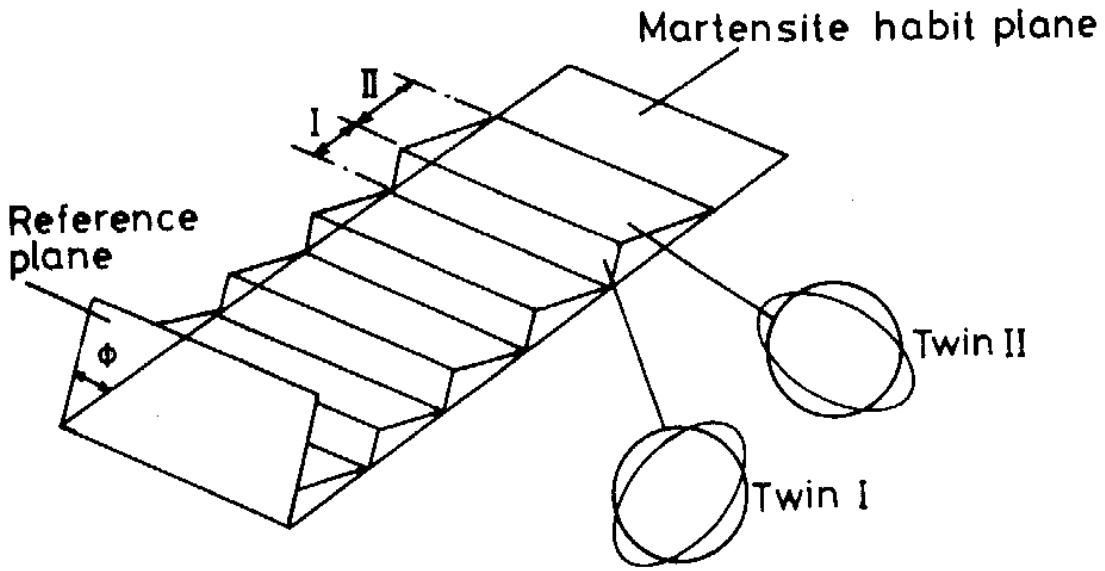

Fig. 6.10 Twins in martensite may be self-accommodating and reduce energy by having alternate regions of the austenite undergo the Bain strain along different axes.

*Slide courtesy of AD Rollett

Atomic model - the Bain Model

- For the case of fcc Fe transforming to body-centered tetragonal (bct) ferrite (Fe-C martensite), there is a basic model known as the Bain model.
- The essential point of the Bain model is that it accounts for the structural transformation with a *minimum of atomic motion*.
- Start with two fcc unit cells: contract by 20% in the z direction, and expand by 12% along the x and y directions.

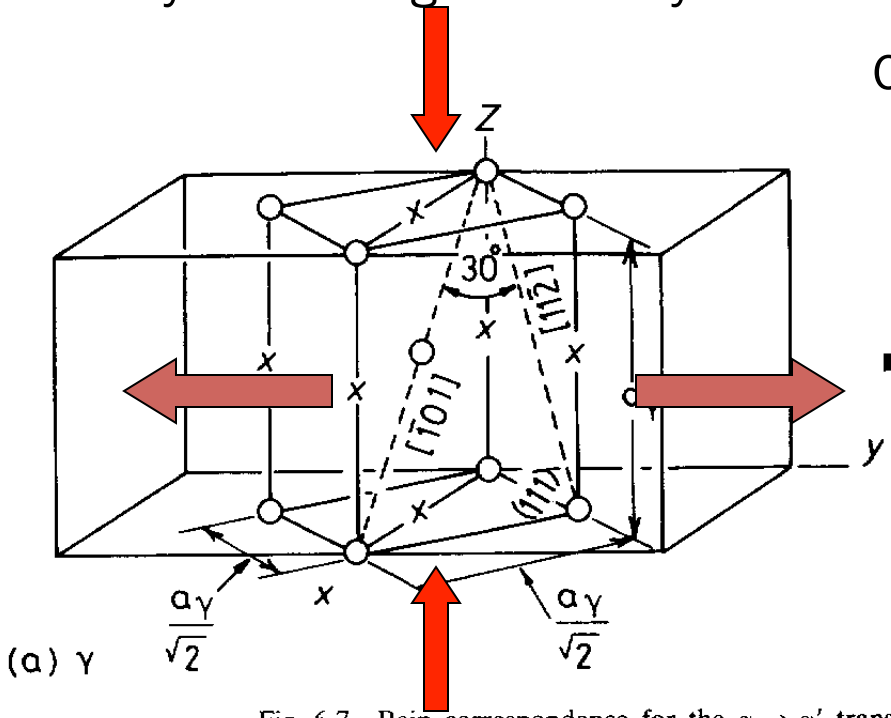

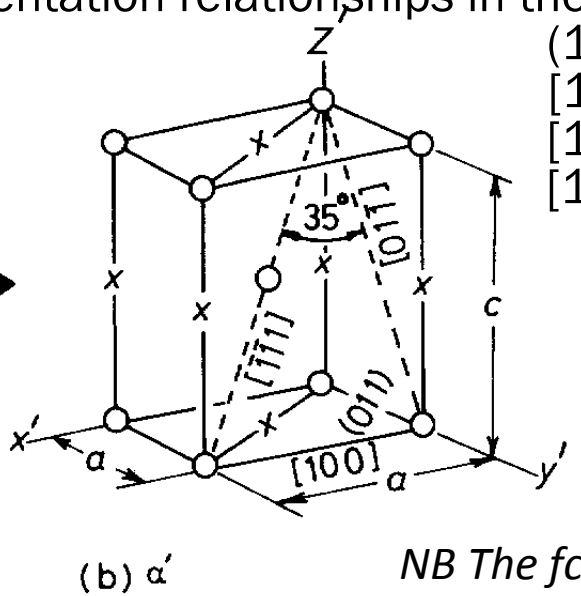

Fig. 6.7 Bain correspondence for the $\alpha \rightarrow \alpha'$ transformation. Possible interstitial sites for carbon are shown by crosses. To obtain α' the γ unit cell is contracted about 20% on the C axis and expanded about 12% on the a axes.

Orientation relationships in the Bain model are:

$(111)_\gamma$ <=> $(011)_{\alpha'}$
$[101]_\gamma$ <=> $[111]_{\alpha'}$
$[110]_\gamma$ <=> $[100]_{\alpha'}$
$[112]_\gamma$ <=> $[011]_{\alpha'}$

NB The fcc lattice can be obtained from the bcc lattice by expanding in the vertical direction by a factor of √2.

*Slide courtesy of AD Rollett

Crystallography, contd.

- Although the Bain model explains several basic aspects of martensite formation, additional features must be added for complete explanations (not discussed in detail here).
- The missing component of the transformation strain is a rotation and an additional twinning shear that changes the character of the strain so as to account for the experimental observation of an *invariant [undistorted] plane*. This is explained in figs. 6.8 and 6.9 and the accompanying text.
- A rather better explanation can be found in *Physical Metallurgy* by P. Haasen, pp 337-343. The best approach to the problem puts it into the form of an *eigenvalue equation*, with transformation matrices to describe each of the 3 component steps of the transformation.

*Slide courtesy of AD Rollett

Role of Dislocations

- Dislocations play an important, albeit hard to define role in martensitic transformations.
- Dislocations in the parent phase (austenite) clearly provide sites for heterogeneous nucleation.
- Dislocation mechanisms are thought to be important for propagation/growth of martensite platelets or laths. Unfortunately, the transformation strain (and invariant plane) does not correspond to simple lattice dislocations in the fcc phase. Instead, more complex models of interfacial dislocations are required.

*Slide courtesy of AD Rollett

Application where OR is important – Accumulated Roll Bonding

Radiation damages bulk crystalline materials

Nanocomposites with high content of certain interfaces are radiation tolerant

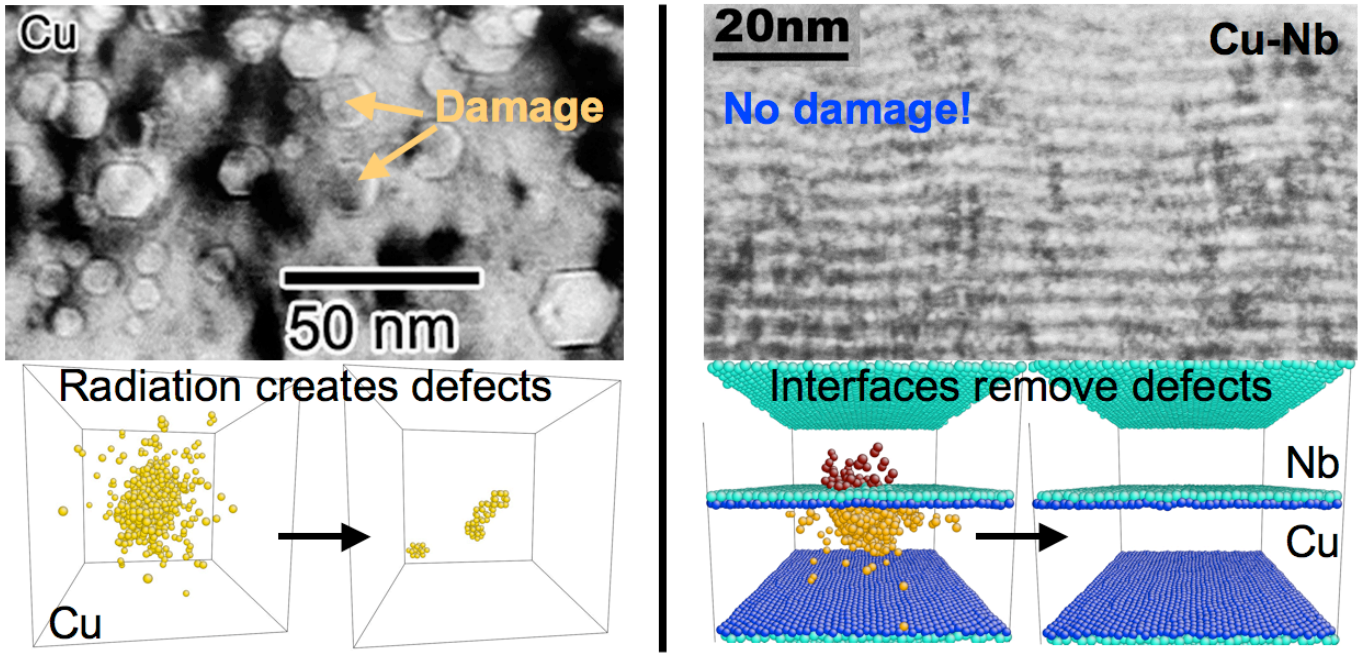

After 33keV He^+ bombardment to ~7dpa

- In layered Cu-Nb composites, Kurdjumov-Sachs interface plays an important role, can act as "super sink" to store radiation induced damages, trapping and recombining defects at the interface
  - Point defect formation energies are order of magnitude lower and rates of Frenkel pair annihilation significantly higher at interfaces than neighboring crystalline layers
    - –Heal damage by trapping and recombining defects before clustering can take place

*Slide courtesy of AD Rollett

A. Misra, M. J. Demkowicz, X. Zhang, R. G. Hoagland, JOM **60**, 62 (2007)

770 nm as-rolled, EBSD

HIPD Results – ARB

HIPD = Heterophase Interphase Plane Distribution

Cu: FCC

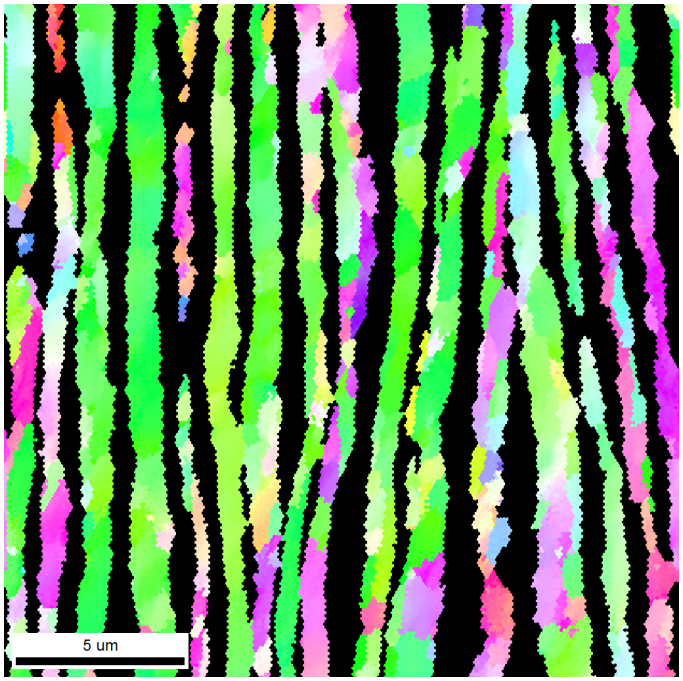

Nb: BCC

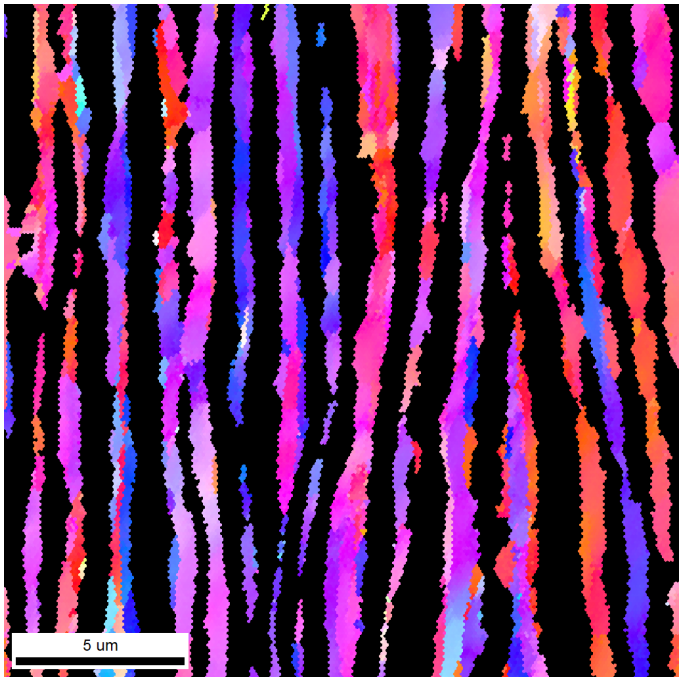

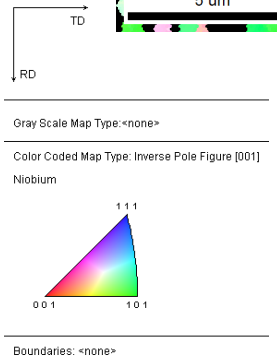

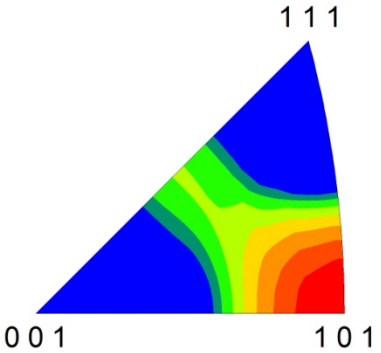

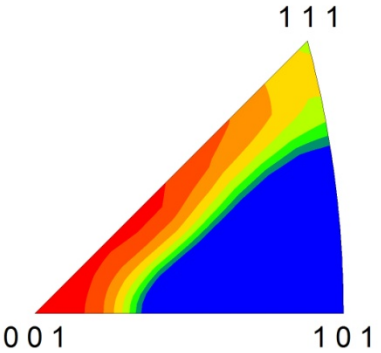

*Slide courtesy of AD Rollett

Samples scanned at Los Alamos.

HICD Results - ARB (KS)

Minimum axis-angle pair, 42.85° <0.968 0.178 0.178>

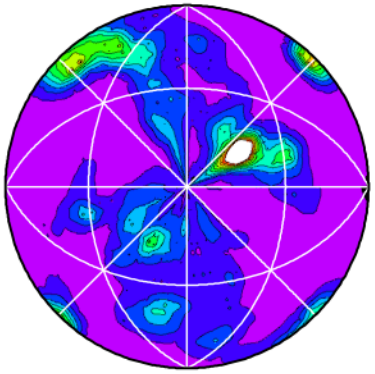

44.88 (max MRD)

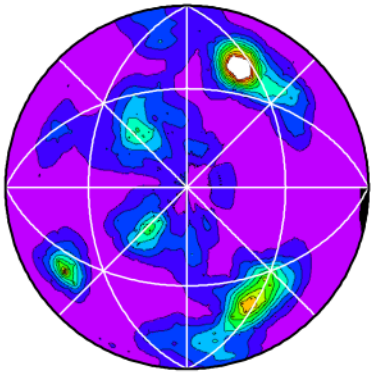

45.68 (max MRD)

001 standard stereographic projection

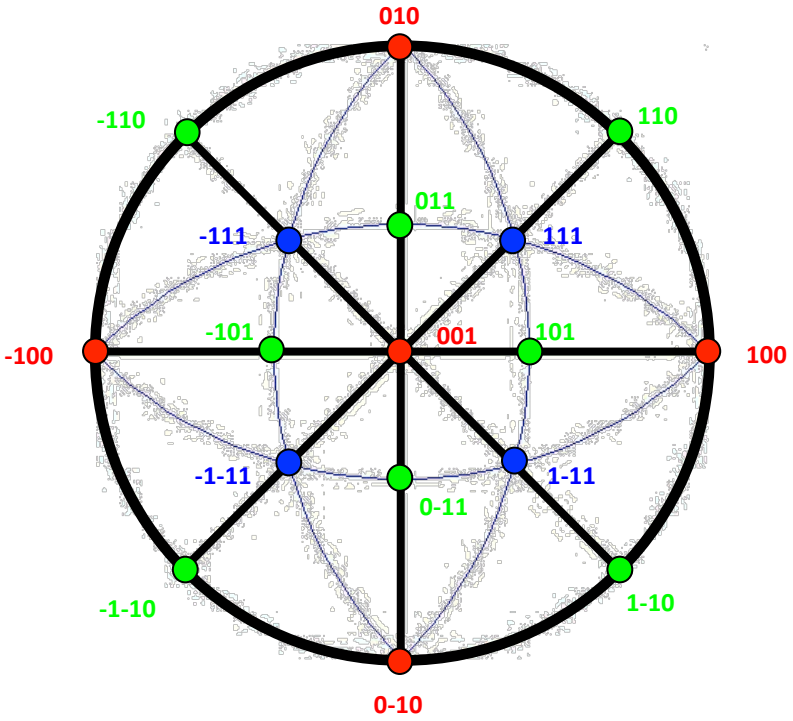

770 nm as-rolled, EBSD

Acta Mater. **59** (2011) 7744; Demkowicz & Thilly; 7° tilt away from ideal {112}//{112} lowers interface energy from 820 down to 690mJ/m^{-2}

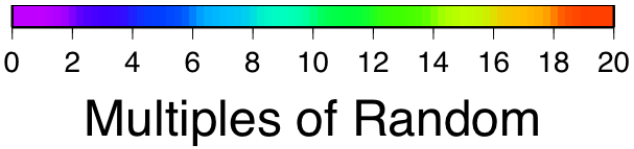

*Slide courtesy of AD Rollett

Ex Situ Thermal stability Study of ARB Cu-Nb (18nm)

- Used drop furnace – each sample held for 1 hr at temperature in vacuum (10^{-7} Torr) and then furnace cooled
- Compare to conventional K-S ({111}Cu//{110}Nb) interface, {112} K-S is high energy interface, is it thermally stable?
- Does the interface deviate from {112} K-S stable?
- Is a triple junction stable?
- Is a very thin layer stable?

*Slide courtesy of AD Rollett

{112} K-S interface is thermally stable

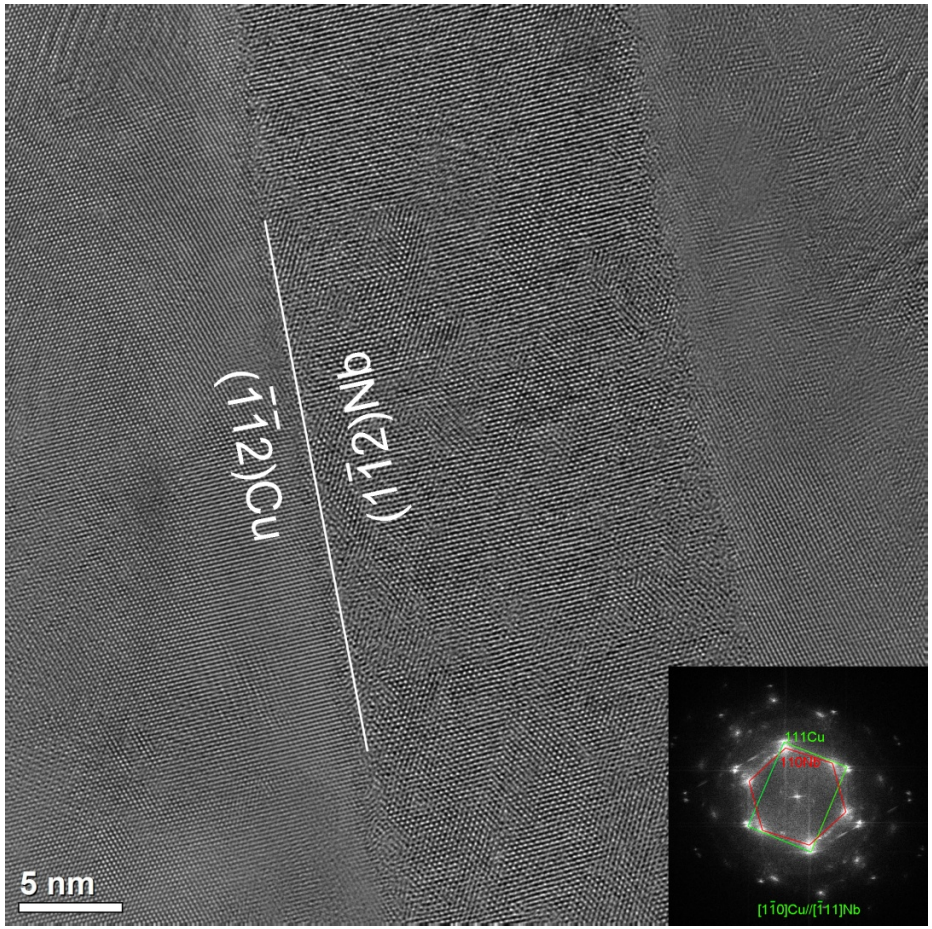

Interfaces that deviate from {112} K-S thermally unstable

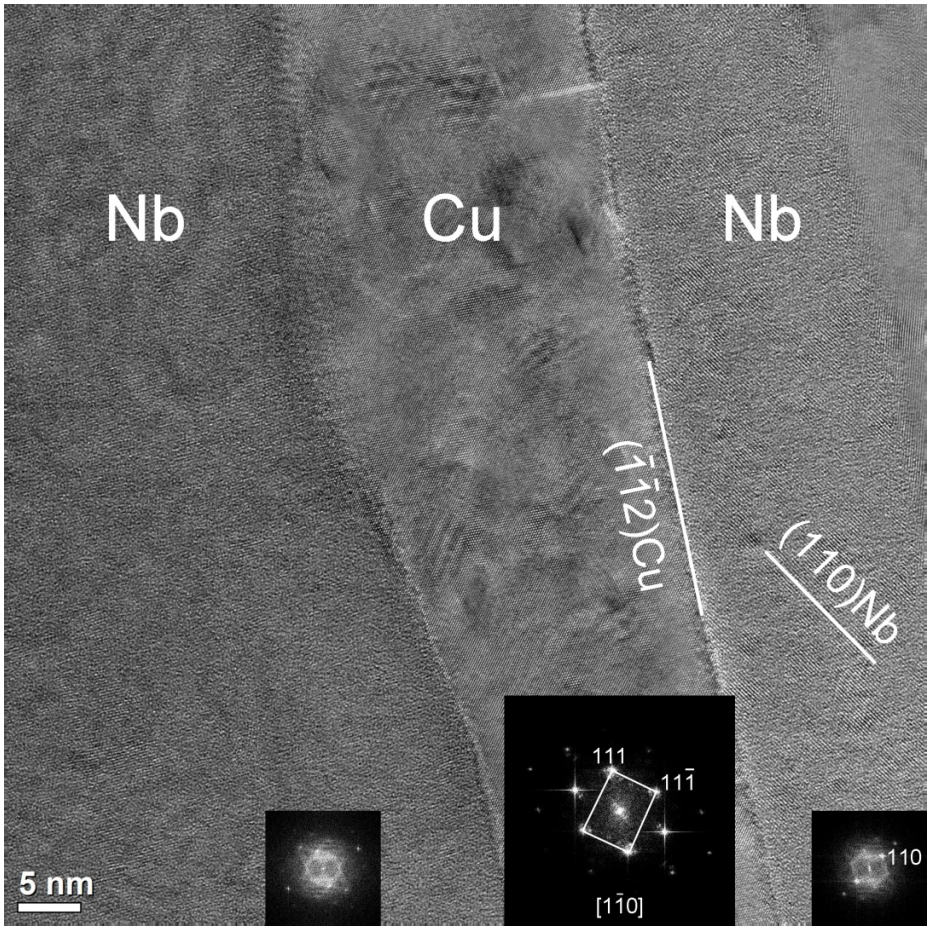

*Slide courtesy of AD Rollett

Summary

- Specific OR exists between product and parent phases for most of the transformations
- Construction of misorientation matrix given an OR is straight-forward given parallel (hkl) [uvw]
- ORs shown to play significant role in many material applications
- Some variants of an OR may be preferred over others depending on mechanism